

**DESIGN, CONSTRUCTION AND TESTING OF AN I-V TESTER
FOR THIN-FILM SOLAR CELLS AND MINI-MODULES**

MAUNG AUNG NAING TUN

(B. Eng, NUS)

A THESIS SUBMITTED

FOR THE DEGREE OF MASTER OF ENGINEERING

DEPARTMENT OF ELECTRICAL AND COMPUTER ENGINEERING

NATIONAL UNIVERSITY OF SINGAPORE

2011

ABSTRACT

In this project, a cost-effective but highly versatile and powerful current-voltage (I - V) tester for thin-film solar cells and modules was designed, constructed, and thoroughly tested. The I - V tester is able to measure thin-film modules with a size of up to 30 cm x 40 cm. The I - V tester uses steady-state illumination from a high-powered xenon lamp and is able to measure I - V curves at light intensities in the 0.001 to 1.2 suns range. The tester is also able to measure short-circuit current density vs. open-circuit voltage (J_{sc} - V_{oc}) curves and dark I - V curves. Using water cooling technology, the solar cell or module temperature is kept constant at a user-defined value in the range of 20-60 °C. The measured curves are analyzed by a computer program built into the tester, yielding important device parameters such as the solar cell/module photovoltaic efficiency, fill factor, series and shunt resistances, and the voltage dependent diode ideality factor.

ACKNOWLEDGMENTS

This thesis would not have been possible without the help of many people. I would like to take this opportunity to express my gratitude and appreciation here.

First, I would like to thank Prof. Armin ABERLE, my main supervisor, for his continuous support and help throughout my research work. Next, I would like to thank Dr. Bram HOEX, my co-supervisor, for his great help, inspiration and supervision of this project. Both provided me with valuable insight to make sure I am on the right research path. I am very grateful for all their advice and guidance during their very tight schedule.

I would also like to thank Dr. Per Ingemar WIDENBORG, Dr. Jidong LONG, Dr. Premachandran VAYALAKKARA, Ms. Juan WANG and Mr. Jonathan ZHANG from the Solar Energy Research Institute of Singapore (SERIS) and consultant Dr. Luc FEITKNECHT for sharing their invaluable expertise, user experience and background knowledge. I am also grateful for Mr. Yu Chang WANG and Mr. Larry QIU from Industrial Vision Technology Pte Ltd and their team for their collaboration with SERIS and great technical support for the successful construction of the T-Sunalyzer system.

It was a pleasure working with many talented graduate students and staff from SERIS, especially the PV Characterization group and I would like to thank them for their discussions and support and friendship.

Last but not the least, I would like to express my gratitude towards my family, friends, managers and colleagues for their encouragement, love, understanding and unconditional support over the years for successful completion of the M.Eng course.

CONTENTS

| | |
|---|----|
| ABSTRACT | i |
| ACKNOWLEDGEMENTS | ii |
| LIST OF FIGURES | vi |
| | |
| CHAPTER 1: INTRODUCTION | 1 |
| | |
| 1.1 Background | 2 |
| | |
| 1.2 Aim of project and thesis | 6 |
| | |
| 1.3 Outline of thesis | 7 |
| | |
| CHAPTER 2: LITERATURE REVIEW | 8 |
| | |
| 2.1 I-V characterization of Solar or Photovoltaics (PV) cells | 9 |
| 2.1.1 Equivalent circuit and characteristic equation | 9 |
| 2.1.2 Characterization parameters | 10 |
| 2.1.2.1 <i>Efficiency</i> | 10 |
| 2.1.2.2 <i>Quantum efficiency</i> | 11 |
| 2.1.2.3 <i>Open-circuit voltage (VOC) and short-circuit current (ISC)</i> | 12 |
| 2.1.2.4 <i>Fill Factor</i> | 12 |
| 2.1.2.5 <i>Series resistance</i> | 13 |
| 2.1.2.6 <i>Shunt resistance</i> | 13 |
| 2.1.2.7 <i>Cell temperature</i> | 14 |
| 2.1.2.8 <i>Reverse saturation current</i> | 15 |
| 2.1.2.9 <i>Ideality factor</i> | 15 |
| 2.1.2.10 <i>Effect of physical size</i> | 16 |
| | |
| 2.2 I-V measurement methods for solar cells | 17 |
| 2.2.1 Electronics | 17 |
| 2.2.2 Illumination Source | 21 |
| 2.2.3 Temperature Control | 23 |
| 2.2.3 Probing Mechanism | 24 |

| | |
|--|----|
| CHAPTER 3: DESIGN AND FEATURES OF T-SUNALYZER | 26 |
| 3. 1 Hardware | 26 |
| 3.1.1 Customized 4-Wire Probe Bars and Micro-Probes | 28 |
| 3.1.2 Electronic Measuring Module | 29 |
| 3.1.2.1 Keithley Model-7708 Differential Multiplexer | 30 |
| 3.1.2.2 Keithley Model-2700 Digital Multimeter | 33 |
| 3.1.2.3 Keithley Model-2425 Source Meter | 35 |
| 3.1.3 Xenon Light Source System | 39 |
| 3.1.4 Thermally Controlled Sample Holder | 42 |
| 3.1.5 Motorized Height Adjuster for Sample Holder | 44 |
| 3.2 Software | 46 |
| 3.2.1 Illumination Test | 47 |
| 3.2.2 Dark Test | 48 |
| 3.2.3 Resistance Test | 49 |
| 3.2.4 Temperature Coefficient Test | 49 |
| 3.2.5 Variable Illumination Measurement (VIM) Test | 50 |
| CHAPTER 4: EXPERIMENTAL SETUP AND MEASURED RESULTS | 51 |
| 4.1 Illumination Test | 53 |
| 4.2 Dark Test | 55 |
| 4.3 Resistance Test | 57 |
| 4.4 Temperature Coefficient Test | 58 |
| 4.5 Variable Illumination Measurement (VIM) Test | 59 |
| CHAPTER 5: CONCLUSION AND RECOMMENDATION | 61 |
| 5.1 Summary and Implications of Measured Results | 61 |
| 5.2 Recommending for Future Works | 64 |
| REFERENCES | 67 |

LIST OF FIGURES

| | |
|---|----|
| Figure 1.1: Transformation of the Global Energy Supply System Towards Sustainability | 2 |
| Figure 2.1: Equivalent Circuit of a Solar Cell | 9 |
| Figure 2.2: Internal quantum efficiency, external quantum efficiency, and reflectance as a function of the wavelength of a typical crystalline silicon solar cell | 11 |
| Figure 2.3: Effect of Temperature on the I-V Characteristics of a Solar Cell | 14 |
| Figure 2.4: I-V curve showing a higher resolution of second scan | 20 |
| Figure 2.5: The standard AM1.5 spectrum compared with the spectrums from Halogen and Xenon light sources | 22 |
| Figure 2.6: Photo of the front side contact probes in a I-V tester for silicon wafer solar cells | 25 |
| Figure 3.1: High-level block diagram of T-Sunalyzer | 27 |
| Figure 3.2: Customized probe bar with five pairs of 4-wire probes | 28 |
| Figure 3.3: Single-axis adjustable micro-probes | 28 |
| Figure 3.4: Wirings in Electronics Measuring Module of T-Sunalyzer | 29 |
| Figure 3.5: Simplified schematic of Keithley 7708 multiplexer | 30 |
| Figure 3.6: Thermocouple connection to internal temperature reference junction | 31 |
| Figure 3.7: 4-wire RTD connection to Model-7708 | 32 |
| Figure 3.8: Connection to DMM with 4-wire measurement function | 33 |
| Figure 3.9: Algorithm used in temperature-monitored scanning of DMM | 34 |
| Figure 3.10: Operating boundaries of Model-2425 SourceMeter | 36 |

| | |
|---|----|
| Figure 3.11: 4-wire connection of DUT to SourceMeter | 38 |
| Figure 3.12: Source and measure sequence of SourceMeter | 39 |
| Figure 3.13: Xenon light source and integrator lens in T-Sunalyzer | 41 |
| Figure 3.14: Water-cooling temperature control system of DUT holder | 43 |
| Figure 3.15: Servo system and motorized linear motion system | 45 |
| Figure 4.1: T-Sunalyzer in SERIS's characterization lab | 52 |
| Figure 4.2: Measured illuminated I-V and P-V curves | 54 |
| Figure 4.3: Measured dark J-V curve | 55 |
| Figure 4.4: Measured dark J-V curve in semi-log scale | 56 |
| Figure 4.5: Measured dark m-V curve | 57 |
| Figure 4.6: Measured $R_{s.light}$ and $R_{s.dark}$ vs. J_{sc} curves | 58 |
| Figure 4.7: Measured J-V curves at different temperatures | 59 |
| Figure 4.8: Measured V_{oc} - J_{sc} curves at different light intensities In semi-log scale | 60 |
| Figure 4.9: Measured FF- J_{sc} curves at different light intensities In semi-log scale | 60 |

LIST OF TABLES

| | |
|---|----|
| Table 2.1: Solar simulator classification | 21 |
| Table 3.1: Source and measurement ranges of Keithley Model-2425 SourceMeter | 36 |

CHAPTER 1: INTRODUCTION

The International Energy Agency (IEA) projects the global energy demand to increase by 1.5% yearly from 2007 to 2030, with an overall increase of about 40%, in their World Energy Outlook 2009. Today's global energy supply mainly comes from fossil fuels such as coal, oil and natural gas which are major sources of greenhouse gases. The Earth's climate will be jeopardized if we continue depending on these fuels without scalable replacements. On the other hand, the actions to reduce carbon emissions could undermine the current global energy system [1].

Since the current energy system is unsustainable, it needs a transformation to a sustainable global energy supply system. Based on a number of studies, a sustainable global energy system is technically and economically achievable. According to BLUE Map scenario in the IEA's 2008 Energy Technology Perspectives Report, solar energy will account for 11% of total primary world energy in 2050. The German Advisory Council on Global Change (WBGU)'s Special Report 2003 expects a greater role of renewable energies in the future and solar electricity is expected to become the most important global energy source by contributing about 20% of world energy supply by 2050 and over 60% by 2100 (Figure 1.1) [2]. This suggests that solar photovoltaics (PV) has a great potential for a sustainable energy economy, and the further development of PV science and technology becomes very crucial for it to become a major electricity and energy source.

WBGU's World Energy Vision 2100

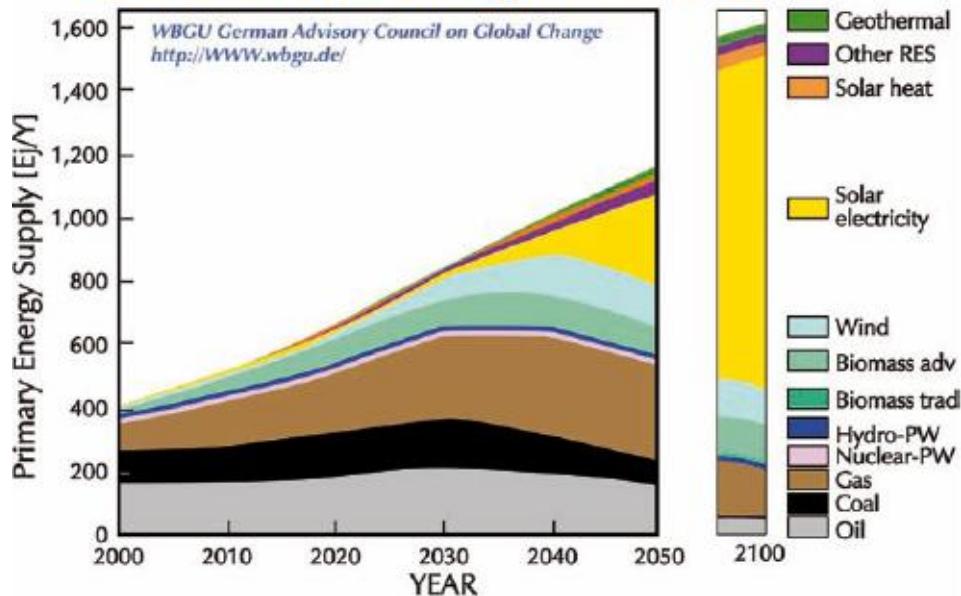


Figure 1.1: Transformation of the global energy supply system towards sustainability. Strict and comprehensive sustainability criteria are applied. This scenario provides the chance to keep global concentrations of CO₂ below 450 ppm. Strong worldwide economic growth is assumed. A substantial increase in energy efficiency is implemented. Extensive use of carbon capture and sequestration is required under this scenario as a transitional technology. There is a phase-out of the use of nuclear energy. Only proven, sustainable potentials for renewable energy sources are used. Traded energies are shown in this graph; non-traded energy contributions (like domestic applications of solar, biomass and geothermal sources) are accounted for under 'energy efficiency' (WBGU, 2003) [2].

1.1 Background

The market development programs to promote the deployment of sustainable energy options and increasing fossil fuel prices have accelerated the growth of solar PV industry. The generation or €/Wp costs are the key challenges for the rapid and large-scale development PV systems. The incremental cost reductions will be achieved with higher conversion efficiency, less material consumption, application of cheaper materials, innovative manufacturing, mass production and optimized system

technology. The proposed priority PV R&D topics needing further study as summarized by The International Science Panel on Renewable Energies (ISPRES) at the end of 2009 include optimization of transparent conductive oxide for thin-film PV, optical concentrating PV, self-organization and alignment in solar cell production using novel concepts and life cycle assessment [2]. Today's mainstream PV technology is based on robust and proven crystalline silicon wafers which seem to have limited cost reduction potential due to the high cost of silicon wafers. In contrast, thin-film PV has a higher potential of cost reduction due to significantly reduced semiconductor material consumption and the ability to fabricate the solar cells on inexpensive, large-area foreign substrates and to monolithically series-connect the fabricated solar cells [3].

Thin-film solar cells are constructed of various thin layers or films of photovoltaic materials on a foreign substrate. The thickness of the layers ranges from a few nanometers to tens of micrometers. Compared to silicon wafer silicon cells, thin film technologies require significantly less active materials to build solar cells. The main advantages of thin film cells are reduced manufacturing cost, potentially lighter weight, flexibility and ease of integration. Thin-film PV is an important technology for building-integrated photovoltaics (BIPV), vehicle PV rooftop or solar chargers for mobile devices. In the long run, it is foreseen that thin-film PV technology will outperform the current solar PV technologies in terms of achieving the cost parity objectives [4].

Amorphous silicon based thin-film PV modules have been in the market for more than 20 years. However, the current market is dominated by CdTe (cadmium telluride) PV modules. The main issues of the CdTe technology are related to the toxicity of Cd and the scarcity of Te. The recent industrial developments have propelled towards CIGS (copper indium gallium diselenide) PV technology and its major technical issue is related to the CIGS absorber layer. It is a complex mixture of five elements being Cu, In, Ga, Se, and S. Other issues are the use of cadmium and the scarce element indium. Microcrystalline silicon cells are not commercially viable at present due to high production cost. Their industrial relevance is improved by combining them with thin a-Si: H cells, forming tandem or so-called micromorph solar cells. A higher PV efficiency is achieved from a better utilization of the solar spectrum due to the large difference in the bandgap values of the two semiconductors (about 1.0 eV and 1.7 eV) [3].

Current-voltage (I - V) testers, which can determine the electrical parameters of solar cells, are used for the design optimization and long-term performance evaluation of photovoltaic devices and modules. The knowledge of the illuminated cell parameters such as short-circuit current density (J_{sc}), open-circuit voltage (V_{oc}), fill factor (FF), series resistance R_s , ideality factor (n) and saturation current density (J_0) is indispensable for the device engineers for the optimization of the cell design. For system engineers, speedy sample handling and I - V measurement techniques are

required to fabricate PV modules with predefined specifications out of a large number of solar cells with non-identical I - V characteristics [5].

A number of I - V tester designs for solar cell measurements are documented in the literature [5-9]. The design concepts are different from each other depending on a wide range of requirements for different types of solar cells concerning accuracy, speed, light source, the positioning of the contacts and cell temperature stability. None of the present commercially available solutions seems specifically designed for productive and efficient research work in optimizing thin-film solar cells as well as for testing them in production lines during the manufacturing process. Therefore, a cost-effective but highly versatile and powerful I - V tester for thin-film solar cells is required by the PV community.

The Solar Energy Research Institute of Singapore (SERIS), in conjunction with a local company (IVT Solar Pte Ltd), developed an I - V tester for silicon wafer solar cells in 2009. It is based on the paper “SUNALYZER - a powerful and cost-effective solar cell I - V tester for the photovoltaic community” by Aberle *et al.* [5], presented at the 25th IEEE Photovoltaic Specialists Conference in Washington D.C. in May 1996. SERIS also has a need for a versatile I - V tester for its thin-film solar cells and modules, but such a system is not commercially available yet. In this project, a cost-effective but highly versatile and powerful I - V tester, thin-film Sunalyzer or T-SUNALYZER, for thin-film solar cells and modules is designed, constructed, and thoroughly tested.

1.2 Aim of the project and thesis

The main objective of the T-Sunalyzer is to measure and analyze I - V characteristics of thin-film solar modules produced by SERIS and some of its research collaboration partners from academia and industry. The in-house design will reduce the overall system cost for SERIS and will also give the flexibility to customize system configuration according to the future needs. Another objective of designing the T-Sunalyzer is to sell the system as a commercial product to other thin-film module research labs and manufacturers in the global PV community.

The T-Sunalyzer was designed to measure thin-film cells and mini-modules with a size of up to 30 cm x 40 cm. It is able to measure I - V curves in the dark and for light intensities in the 0.001 to 1.2 suns range. This enables the determination of various cell parameters as a function of the light intensity, which yields valuable information for thin film solar cell researchers. The important device parameters such as the solar cell/module efficiency, fill factor, series and shunt resistances, and the voltage dependent diode ideality factor are automatically provided by the T-Sunalyzer by analyses of the measured I - V curves with a computer program. This thesis documents the research work during the design stage, the hardware and software design blocks and the main features of the T-Sunalyzer, debugging and troubleshooting work during the construction stage and experimental results of measurements for thin film solar cells or modules.

1.3 Outline of thesis

The thesis is arranged as follows. Chapter 2 primarily gives a review of the basic principles and characterization aspects of solar cells and I - V measurement techniques. The various light sources used in the I - V testers and temperature control techniques for the solar cells during the measurements are also presented. The related research works from other researchers are reviewed.

Chapter 3 concerns with the design and implementation of the T-Sunalyzer. The Chapter starts with the introduction of the proposed I - V tester specifications. It is followed by high level design and hardware design of all major blocks of the T-Sunalyzer. The structure of the light source and new design idea for controlling the temperature of the solar cells will be described. The Chapter concludes with the design considerations and user interface aspects of the T-Sunalyzer.

Chapter 4 presents experimental results obtained with the T-Sunalyzer. The performance of T-Sunalyzer at different light intensities will be presented. The measurement results will be compared with literature data.

In Chapter 5, the main conclusions of this work will be presented together with some suggestions for future work.

CHAPTER 2: LITERATURE REVIEW

The T-Sunalyzer is designed for I - V characterization of thin-film solar cells or mini-modules and determination of efficiency and other device parameters. For an ideal solar cell, the efficiency depends on the light-generated current and the recombination of electrons and holes via the Shockley-Read-Hall (SRH) process and other processes in the solar cell. But, the detrimental mechanisms such as series resistance and shunt resistance limit a solar cell from achieving its ideal efficiency. The measurements and analysis of I - V curves help the researchers to understand the detrimental mechanisms for lower efficiency.

The I - V curve of an ideal solar cell is exponential. The displacement along the I-axis depends on the light-generated current and its shape depends on the dominant recombination mechanism. The I - V curve of a real solar cell is distorted by one or more detrimental mechanisms and is more difficult to analyze. The local ideality factor vs. voltage (n - V) curve which is related to the differential of the I - V curve is normally generated to get more information about the I - V curves. By studying I - V curves, researchers can devise fabrication procedures to alleviate the influence of the various mechanisms, such as edge recombination, resistance-limited enhanced recombination, floating-junction shunting and series resistance, on the efficiency in an economically relevant process [10]. This chapter mainly discusses the equivalent

circuit and characteristic equation of a solar cell, I - V characterization parameters and I - V measurement methods for solar cells/modules.

2. 1 I-V characterization of Solar cells

2.1.1 Equivalent circuit and characteristic equation of a solar cell

The electrically equivalent model of an ideal solar cell includes a current source in parallel with a diode. The current source represents the photo-generated current and the diode represents the p - n junction. But, no solar cell is ideal in practice and the shunt and series resistance are added to the model resulting in the one-diode equivalent circuit shown in Figure 2.1 [11].

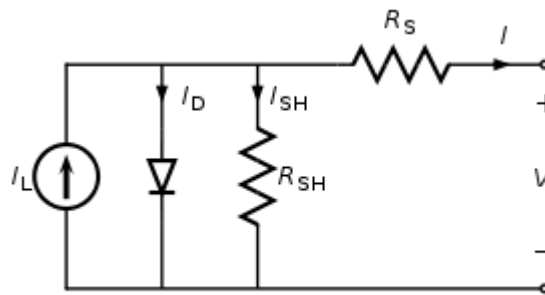


Figure 2.1: One-diode equivalent circuit of a solar cell

From the equivalent circuit, the current produced by solar cell is equal to:

$$I = I_L - I_D - I_{SH}, \text{ where} \quad (2.1)$$

I = output current

I_L = photogenerated current

I_D = diode current.

$$I_{SH} = \text{shunt current} = \frac{V+IR_S}{R_{SH}}$$

The diode current equation is given by

$$I_D = I_0 \left\{ \exp \left[\frac{qV_D}{nkT} \right] - 1 \right\} = I_0 \left\{ \exp \left[\frac{q(V+IR_S)}{nkT} \right] - 1 \right\}, \text{ where} \quad (2.2)$$

I_0 = reverse saturation current

n = diode ideality factor (1 for an ideal diode)

q = elementary charge

k = Boltzmann's constant

T = absolute temperature; at 25°C, $\frac{kT}{q} \approx 0.0259$ volts

So the characteristic equation of a solar cell can also be rewritten as:

$$I = I_L - I_0 \left\{ \exp \left[\frac{q(V+IR_S)}{nkT} \right] - 1 \right\} - \frac{V+IR_S}{R_{SH}}. \quad (2.3)$$

2.1.2 Characterization parameters

2.1.2.1 Efficiency

The energy conversion efficiency (η) of a solar cell represents the ratio electrical energy generated and the incident energy of the used light source.

Mathematically, it is the maximum power point (P_m in W/m^2) divided by the input light irradiance (P_{light} in W/m^2) [12].

$$\eta = \frac{P_m}{P_{\text{light}}} \quad (2.4)$$

As η is dependent on e.g. the light intensity, spectrum of the light source and the temperature, it is necessary that all solar cells are measured under identical conditions to compare results obtained in different labs. The standard test

conditions (STC) are defined as a fixed cell temperature 25 °C and an irradiance of 1000 W/m² with air mass of 1.5 (AM1.5) spectrum.

2.1.2.2 Quantum efficiency

The external quantum efficiency (EQE) of a solar cell is the ratio of number of carriers collected by the solar cell to the number of incident photons of a given energy. The EQE as a function of wavelength of a silicon wafer solar cell is shown in Figure 2.2. In some instances, some of the photons reaching the cell are reflected, or some pass through the cell and are transmitted. The EQE can be measured experimentally. By taking into account reflection and transmission losses, internal quantum efficiency (IQE) can be derived [13].

$$IQE = \frac{EQE}{1-R-T} \quad (2.5)$$

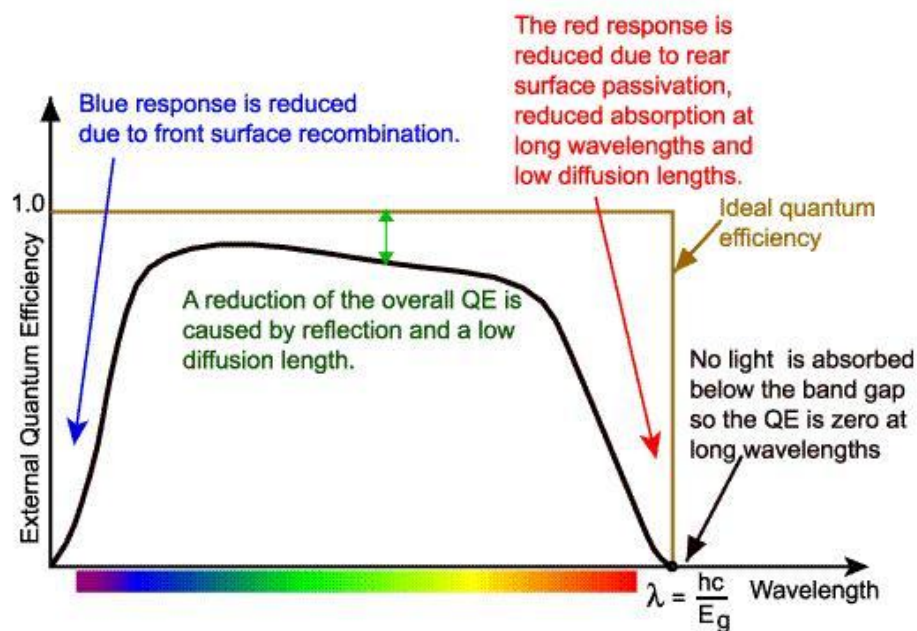


Figure 2.2: External quantum efficiency as a function of the wavelength of a silicon solar cell [13].

The measured EQE is corrected with the measured R to calculate the IQE. If the active layer of solar is unable to convert the absorbed photons efficiently, a low IQE is the result. The ideal IQE curve is square, with a 100% QE above the semiconductor bandgap energy. Typically, an IQE curve is not square due to recombination and parasitic absorption of the incident photons.

2.1.3.3 Open-circuit voltage (V_{OC}) and short-circuit current (I_{SC})

When a solar cell is operated at open circuit, $I = 0$ and the voltage across the output terminals is defined as the open-circuit voltage. Assuming the shunt resistance is high enough to be neglected in the characteristic equation (2.3), the open-circuit voltage V_{OC} is:

$$V_{OC} \approx \frac{kT}{q} \ln \left(\frac{I_L}{I_0} + 1 \right). \quad (2.6)$$

Similarly, when the cell is operated at short circuit, $V = 0$ and the current I through the terminals is defined as the short-circuit current. For a high-quality solar cell with low R_S and I_0 , and high R_{SH} , the short-circuit current I_{SC} is equal to I_L

2.1.3.4 Fill factor

The fill factor (FF) of a solar cell is calculated as the ratio of actual maximum obtainable power, ($V_{mp} \times J_{mp}$) to the maximum theoretical power ($J_{sc} \times V_{oc}$). J_{mp} and V_{mp} refer to current density and voltage at maximum power point. Both values are derived from varying the loading resistance until $J \times V$ is at its highest

value. The fill factor is also considered as one of the most important parameters for the energy production of a photovoltaic cell.

$$FF = \frac{P_m}{V_{OC} \times I_{SC}} = \frac{V_{mp} \times I_{mp}}{V_{OC} \times I_{SC}} \quad (2.7)$$

A higher fill factor results in a higher efficiency and implies that the cell's output power is getting closer to its maximum theoretical value. The higher fill factor ratio can, among others, be achieved by decreasing the series resistance (R_S) and increasing the shunt resistance (R_{SH}) [14].

2.1.3.5 Series resistance

The voltage drop across the R_S depends on the extracted current and can significantly reduce the terminal voltage V . At very high values of R_S , the series resistance dominates and the behavior of the solar cell resembles that of a resistor. Losses caused by series resistance are approximated by $P_{loss} = V_{RS} I = I^2 R_S$ and increase quadratically with the photo-current. So, series resistance losses are the most important at high illumination intensities.

2.1.3.6 Shunt resistance

As the shunt resistance decreases, the current diverted through the shunt resistor increases for a given level of junction voltage. Very low values of R_{SH} will produce a significant reduction in V_{OC} and a badly shunted solar cell will take on operating characteristics similar to those of a resistor.

2.1.3.7 Cell temperature

The temperature most significantly affects I_0 in the characteristic equation of solar cell (2.3). I_D increases exponentially with the applied voltage and the magnitude of the exponent in the characteristic equation reduces with increasing T . The net result is the linear reduction of V_{OC} and this effect is less pronounced for high- V_{OC} solar cells. Due to the slight decrease in the bandgap with increasing T , the photogenerated current (I_L) slightly increases with rising T . The total effect of temperature on the cell efficiency is computed using these factors together with the characteristic equation.

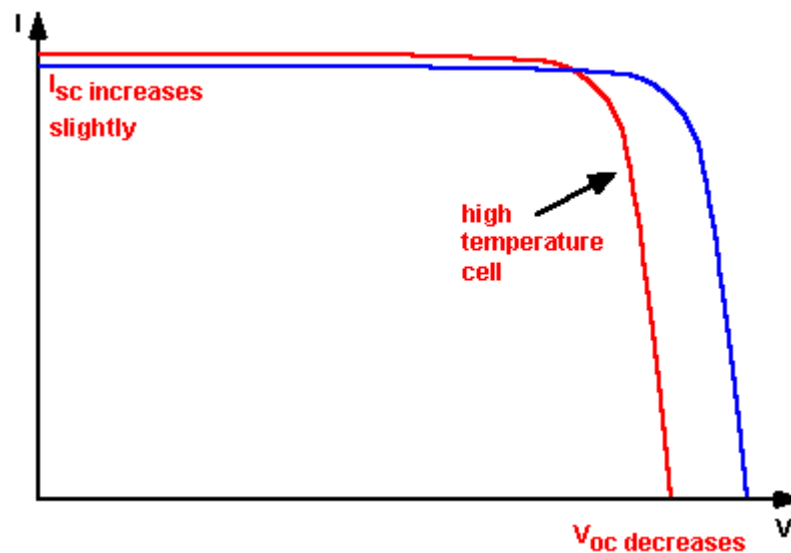


Figure 2.3: Effect of temperature on the I-V characteristics of a solar cell [13].

But, the total effect on efficiency is similar to that on V_{OC} because the change in voltage is much stronger than that on current. The effect of increasing temperature on the I-V curve of a solar cell is shown in Figure 2.3.

2.1.3.8 Reverse saturation current

If an infinite shunt resistance is assumed, the characteristic equation (2.3) can be solved for V_{OC} :

$$V_{OC} = \frac{kT}{q} \ln \left(\frac{I_{SC}}{I_0} + 1 \right) \quad (2.8)$$

Thus, an increase in I_0 produces a reduction in V_{OC} . This explains mathematically the reason for the reduction in V_{OC} that accompanies increases in temperature described in Section 2.1.3.7.

Physically, a reverse saturation current is a measure of the thermally generated carriers in the device when a reverse bias is applied. This leakage is a result of carrier generation in the neutral regions on either side of the junction as well as junction depletion region.

2.1.3.9 Ideality factor

The ideality factor describes the diode's behavior and how closely that matches to the theory's assumption [13]. The ideality factor is a fitting parameter that assumes the p-n junction of the diode is an infinite plane and there is no recombination within the space-charge region. When the diode's behavior fully complies the ideal theory, $n = 1$. On the other hand, when $n = 2$, for example, it means that recombination occurs in the space charge region and dominates other recombination processes.

Solar cells are mostly larger in size compared to conventional diodes and usually exhibit near-ideal behavior ($n \approx 1$) under STC. However, the recombination in the space charge region may dominate the device operation due to the specific operating conditions. This increases I_0 and ideality factor ($n \approx 2$). The change in ideality factor will increase the output voltage of solar cell while an increase in I_0 will decrease it. The change in I_0 is more significant typically and it results a reduction in output voltage.

2.1.3.10 Effect of physical size

The physical size of a solar cell influences I_0 , R_S , and R_{SH} . Assuming a comparison is done on otherwise identical cells, a cell that has twice the surface area of another cell theoretically will have double the value of I_0 and half the values of R_S and R_{SH} . As such, the characteristic equation (2.3) can be described by the current produced per unit cell area or current density as shown below.

$$J = J_L - J_0 \left\{ \exp \left[\frac{q(V + JR_S)}{nkT} \right] - 1 \right\} - \frac{V + JR_S}{R_{SH}}, \text{ where} \quad (2.9)$$

J = current density (amperes/cm²)

J_L = photogenerated current density (A/cm²)

J_0 = reverse saturation current density (A/cm²)

R_S = specific series resistance (Ω -cm²)

R_{SH} = specific shunt resistance (Ω -cm²).

The density equation is useful in comparing cells of different physical dimensions as well as in comparing cells from different manufacturers. It also scales the parameter values towards a similar order of magnitude so that any numerical extraction is simpler and more accurate. But it should only be applied when comparing solar cells that have similar and comparable layout. Very small cells may give higher J_0 and lower R_{SH} as recombination and contamination of the junction is largest at the perimeter of the cells, and these effects should be considered.

2.2 I-V measurement methods for solar cells

Solar cells and modules are developed in a wide range of power level and conversion efficiencies as they are being used in various residential, commercial and military applications. The requirements for measuring speed, accuracy and the range of I - V characteristics also vary depending on research, quality assurance or production purpose. The different electronics, illumination sources, temperature controls, probing mechanisms and software tools are chosen in various solar cell I - V measurement methods in order to optimize the required performance within the targeted budget.

2.2.1 Electronics

An I - V curve of solar cell is typically obtained by stepping the solar cell output loading from I_{sc} to V_{oc} conditions. A set of electronic equipment with a voltage range that covers at least V_{oc} and can sink I_{sc} is required to measure the current at each

loading. Many types of the I - V measurement techniques have been researched and developed for solar cell characterization: 1) power variable resistance method 2) dynamic capacitor charging method; 3) electronic load method; 4) four-quadrant power supply or SourceMeter method and 5) two-quadrant power supply method.

In the power variable resistance method, a set of high-precision resistors or power variable resistances are used as the load of the PV device. The I - V characteristics are obtained by measuring the current as the voltage drops on one of the resistors with different resistance values. A direct measurement of V_{oc} is taken by opening the switching relays for all resistors. The principle of this method is simple, but it takes time to switch the resistors. Only limited data can be obtained and the testing precision is affected [6].

In the dynamic capacitor charging method, a set of capacitors is used as the variable load of the PV device. First, the capacitors are reset to their initial state by discharging the circuit. At the initial stage of charging of the capacitors, the capacitor impedance is very small and the current flowing through the capacitor tank is nearly equal to the short circuit current I_{sc} of the PV device. The charging current approaches zero as the capacitor becomes charged up to the open circuit voltage V_{oc} of the solar array. Thus, the load of the solar device changes from zero to a very large value during the capacitor charging period and I - V characteristics of the solar device is acquired by sampling the current and voltage data. The load control is

simple and fast and continuous measurements can be done with this method. But a fast controlling system and high precision sampling are needed and typically high measurement accuracy is difficult to achieve [7].

In the electronic load method, an electronic load at constant voltage mode is adopted as the load of PV device. The load is controlled by a controller equipped with specific software to step through a range of voltages. At each voltage step, the current is measured. Electronic loads are a good solution for characterizing PV modules because they have a much larger maximum power range compared to DC power supplies and SourceMeters. This method is faster and more accurate than variable resistance and capacitor charging methods but the control software is more complicated because both the load and the data acquisition need to be controlled. The electronic loads cannot sink the current down to 0 V and their maximum current sink capability starts to drop around 3 V. This results in a limitation for *I-V* curve characterization [15].

In research and for quality assurance testing, it is necessary to characterize the *I-V* curve under illuminated conditions. It is also useful to analyze the reverse bias characteristics of the solar cell under dark conditions. To fully characterize a solar cell with a single electronic measurement device, using a four-quadrant DC source or SourceMeter which can source voltage and current as well as measurement capabilities is the simplest method. But they have limited power ratings.

In the two-quadrant power supply method, DC sources that are capable of sourcing and sinking current are used. Two-quadrant sources are unable to produce negative voltages. However, they can be used like four-quadrant sources with simple switching which is built-in for many DC sources. Two-quadrant sources typically do not have the large power range of an electronic load but they can sink current at 0 V and often have better measurement accuracy than an electronic load. The test plan needs to accommodate the discontinuity between the DC source and the solar cell under test during switching. [16].

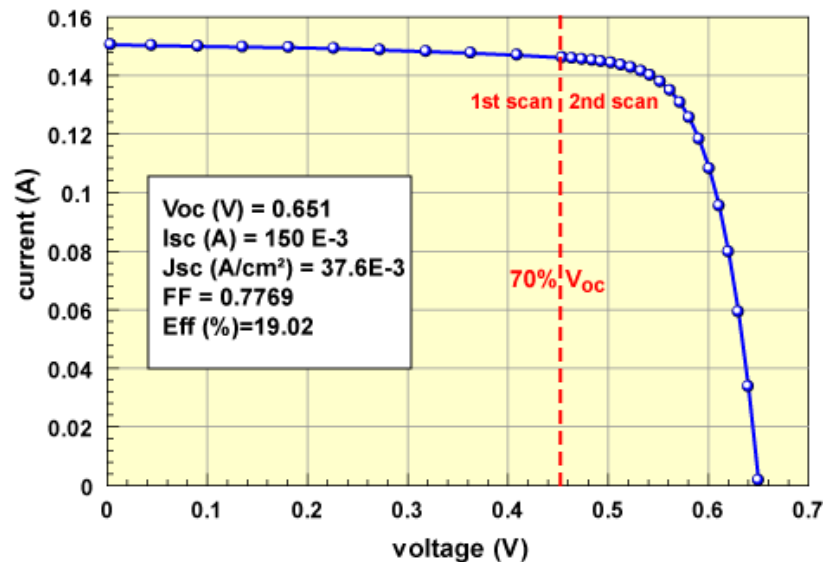


Figure 2.4: I-V curve showing a higher resolution of second scan

The I-V curve has a strongly varying slope and there are various schemes used for improving the accuracy. One of the simplest methods is to take equally spaced measurements in two steps. The first section is widely spaced and covers from 0 to

70 % of V_{oc} . The second section has measurement points more closely spaced and covers from 70 % to V_{oc} . The second region contains the maximum power point, the open circuit voltage and has a much higher slope as shown in Figure 2.4 [17].

2.2.2 Illumination Source

A stable light source that is close to the STC is required to characterize solar cells. The variations in atmospheric conditions and requirement in comparing measurements over time limit the use of the sun itself. Solar simulators are classified according to spectral match, irradiance inhomogeneity (spatial uniformity over the illumination area) and temporal instability (stability over time) and their classification is shown in Table 2.1 where class-A is the best rating [17].

Table 2.1: Solar simulator classification

| Class | Spectral Match | Irradiance inhomogeneity | Temporal Instability | |
|----------|----------------|--------------------------|----------------------|------------|
| | | | Long Term | Short Term |
| A | 0.75 - 1.25% | 2% | 0.5% | 2% |
| B | 0.6 - 1.4% | 5% | 2% | 5% |
| C | 0.4-2.0% | 10% | 10% | 10% |

The most commonly used light source is a xenon arc lamp with suitable lens and filters to approximate the AM1.5G spectrum. In some cases, low budget testers use halogen lamps as the light source. They normally come with a dichroic filter that selectively passes light of a specific range of wavelengths but filtering out the other unnecessary wavelengths. The halogen lamp filament produces much more infrared

light and much less UV compared to the AM1.5 spectrum. Halogen lamps have the advantage of greater temporal stability compared to xenon arc lamps.

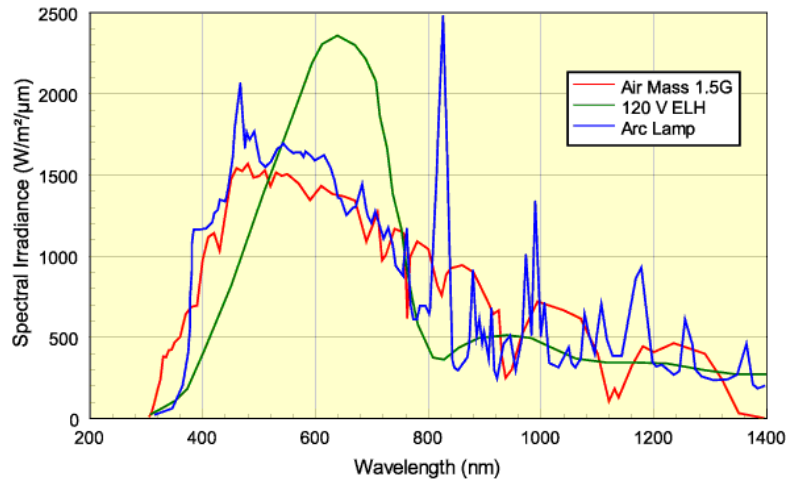


Figure 2.5: The standard AM1.5 spectrum compared with the spectra from halogen and xenon light sources [17].

The main disadvantage of the usage of continuous light solar simulators is the rise of the temperature of the sample during the $I-V$ measurement. This can result in an inaccurate V_{OC} determination. But it can be controlled and reduced to acceptable level with shutters for the light source and a cooling system for solar cells. It may also be corrected in the software.

The deviations from AM1.5 cause errors in I_{sc} . So, $I-V$ testers are normally built with a calibration cell. The light intensity used in the tester can be adjusted to match the I_{sc} of the calibration cell to be same as that measured in an external testing

laboratory. It is also difficult to condition a light source to exactly match the AM1.5 spectrum. The spectral differences will cause current mismatch between junctions in multi-junction PV modules and filtering methods are applied in order to minimize measurement errors.

Another commonly used light source for I - V characterization of solar cells and modules is the flash-type solar simulator. It produces a light pulse with a constant high level of light intensity for a few milliseconds. During this time, the full I - V curve is traced out accordingly [6, 8, and 9]. There are multi-flash systems which use multiple flashes to build up the I - V curve, taking only a single I - V point with each flash. The implementation of flash testers is normally complex, expensive, and susceptible to transient capacitive errors caused by rapid changes of the charge distribution in the cell with high-speed measurements.

2.2.3 Temperature control

One-sun illumination is quite intense and it is important to prevent heating up solar cells as they are sensitive to temperature. Poor temperature control introduces errors in V_{OC} and the error is dependent on the band gap of material. Typically, the sample is placed on a sample holder which is kept at 25 °C by a temperature control system. The rear of many commercial solar cells is covered with metal and has good contacts with the sample holder and thermocouples can be used relatively easily to determine the actual temperature.

However, some solar cells have back contacts and a sophisticated temperature control is required. Flash testers largely eliminate temperature control problems but sophisticated electronics are needed to take measurements quickly and must be synchronized with the flash. Flash testing is also used in the case where direct control of temperature of the sample is impossible due to the encapsulation.

2.2.4 Probing mechanism

Solar cell I - V testing uses four-wire sensing or four-point probe method which uses separate pairs of current-carrying and voltage-sensing electrodes to achieve more accurate measurements than traditional two-wire sensing. The number of probes and the pattern of probe arrays are normally customized based on the cell or module sizes and also based on whether the contacts are on front, back or on both sides of the cell [17]. A number of voltage and current probe pairs are used for the cells as shown in Figure 2.6 because a single voltage and current pair is insufficient.

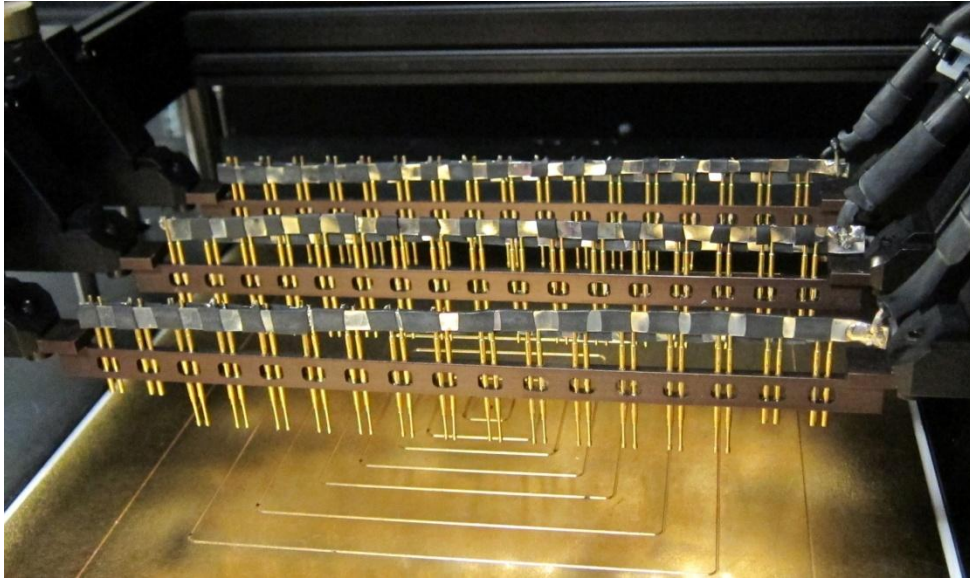


Figure 2.6: Photo of the front side contact probes in an I-V tester for silicon wafer solar cells.

The voltage and current probes are normally assembled close to each other without touching to avoid erroneous measurements. The simple solution to overcome the contact problem is to align the probes on the solar cell slightly and measure again. If one observes significant fluctuations in the fill factor for repeated measurements, this indicates that the probes most likely have contacting problems with the cell.

CHAPTER 3: DESIGN AND FEATURES OF T-SUNALYZER

The T-Sunalyzer was designed with test and measurement building blocks which are assembled together and integrated with control and analysis software in order to meet the technical specifications discussed in the abstract. This reduces the risk of obsolescence in an industry driven by rapidly developing technologies. The system has the capability to exchange the individual blocks as testing requirements change. For example, if the maximum voltage or current range of test requirements is changed in the future, we would need to replace only one of the building blocks of the system, rather than build a new system. The various blocks of the system also can be re-used for other test system platforms, as the design is aimed for standardization and equipment re-use.

3. 1 Hardware

The high-level schematic representation of the T-Sunalyzer is shown in Figure 3.1. In the next sections each component will be discussed in detail.

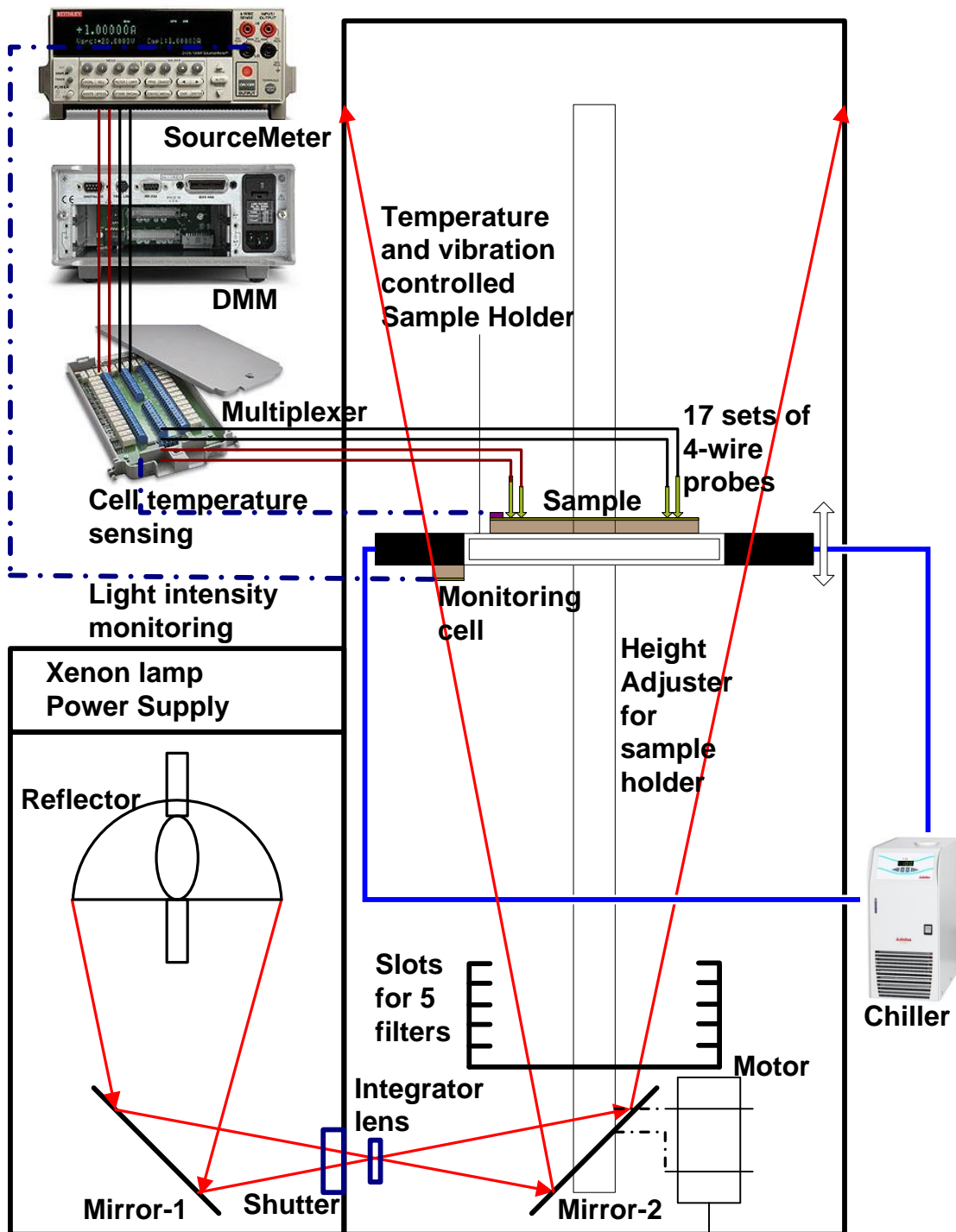


Figure 3.1: High-level block diagram of T-Sunalyzer.

3.1.1 Customized 4-wire probe bars and micro-probes

The T-Sunalyzer probing mechanism is designed to characterize thin-film cells and mini modules on glass sheets with a size of up to 30 cm x 40 cm. The samples are contacted on the upward-facing rear surface to simplify the task of aligning the probes to the contacts. There are three 2-axis adjustable probe bars which are customized based on SERIS' cell layout and each includes five sets of 4-wire probes as shown in Figure 3.2. The individual probes in the probe bars can be easily removed or changed if deemed necessary.

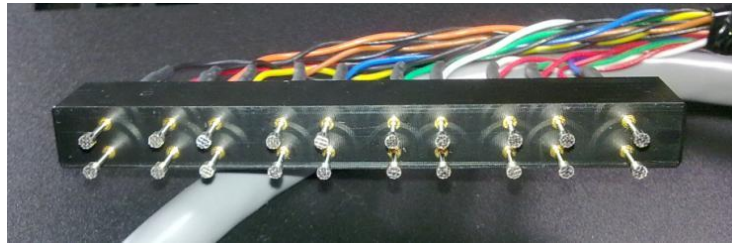


Figure 3.2: Customized probe bar with five pairs of 4-wire probes.

The T-Sunalyzer also includes four pairs of single-axis adjustable micro-probes which give two additional sets of 4-wire probes for characterizing specific types of thin-film solar cells of any pattern as shown in Figure 3.3. The 17 channels of 4-wire probes are connected to a SourceMeter for I-V measurements via a multiplexer and selection of channels is controlled by a digital multimeter (DMM).



Figure 3.3: Single-axis adjustable micro-probes.

3.1.2 Electronic measuring module

The electronic measuring instruments for T-Sunalyzer were chosen to perform I - V measurements from 17 channels of 4-wire probes in the ± 100 V and ± 3 A range, which is well within the expected range of parameters for the thin film solar cells and module structures investigated at SERIS. The intensity and stability of the light source are monitored by measuring the output current from a Si monitoring cell. The ambient temperature and the cell temperature are monitored by a K-type thermocouple and 4-wire resistance temperature detector (RTD) so that I - V measurements can be triggered to start at a temperature of 25 °C. The electronic measuring module mainly includes a differential multiplexer, a digital multimeter (DMM) and a SourceMeter. The wiring between the instruments is shown in Figure 3.4.

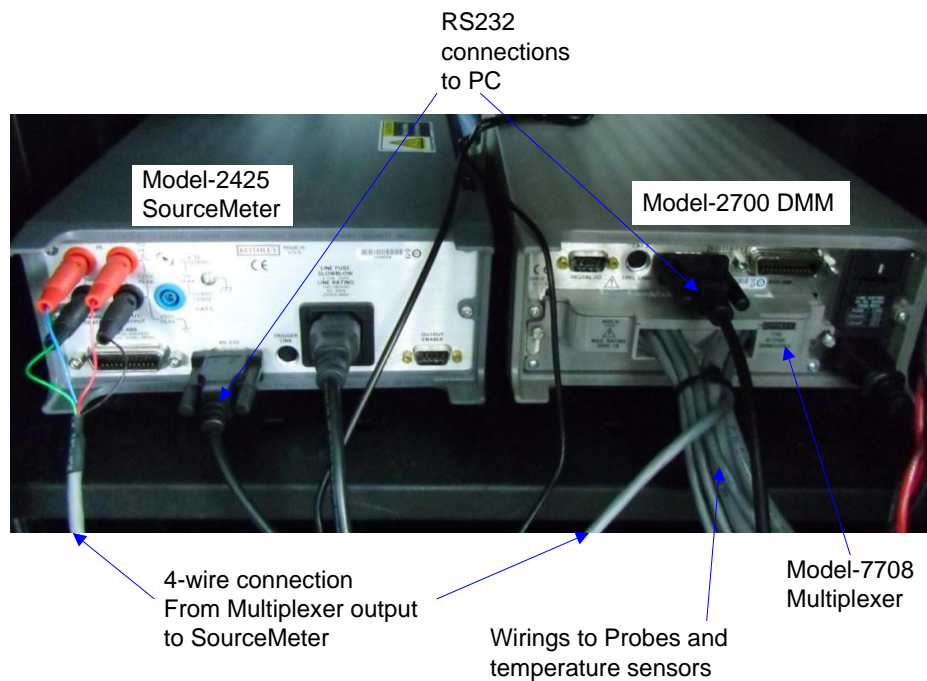


Figure 3.4: Wirings in Electronics Measuring Module of T-Sunalyzer.

3.1.2.1 Keithley Model-7708 differential multiplexer

The Keithley Model-7708 differential multiplexer module is configured as 20 channels of 4-pole multiplexer switching to route the voltage and current signals from 17 channels of 4-wire probes to the SourceMeter. The channels of Model-7708 multiplexer are grouped into two banks as shown in Figure 3.5 and backplane isolation is provided for each bank. The backplane connector provides connections to the Model-2700 DMM which controls the selection of channels.

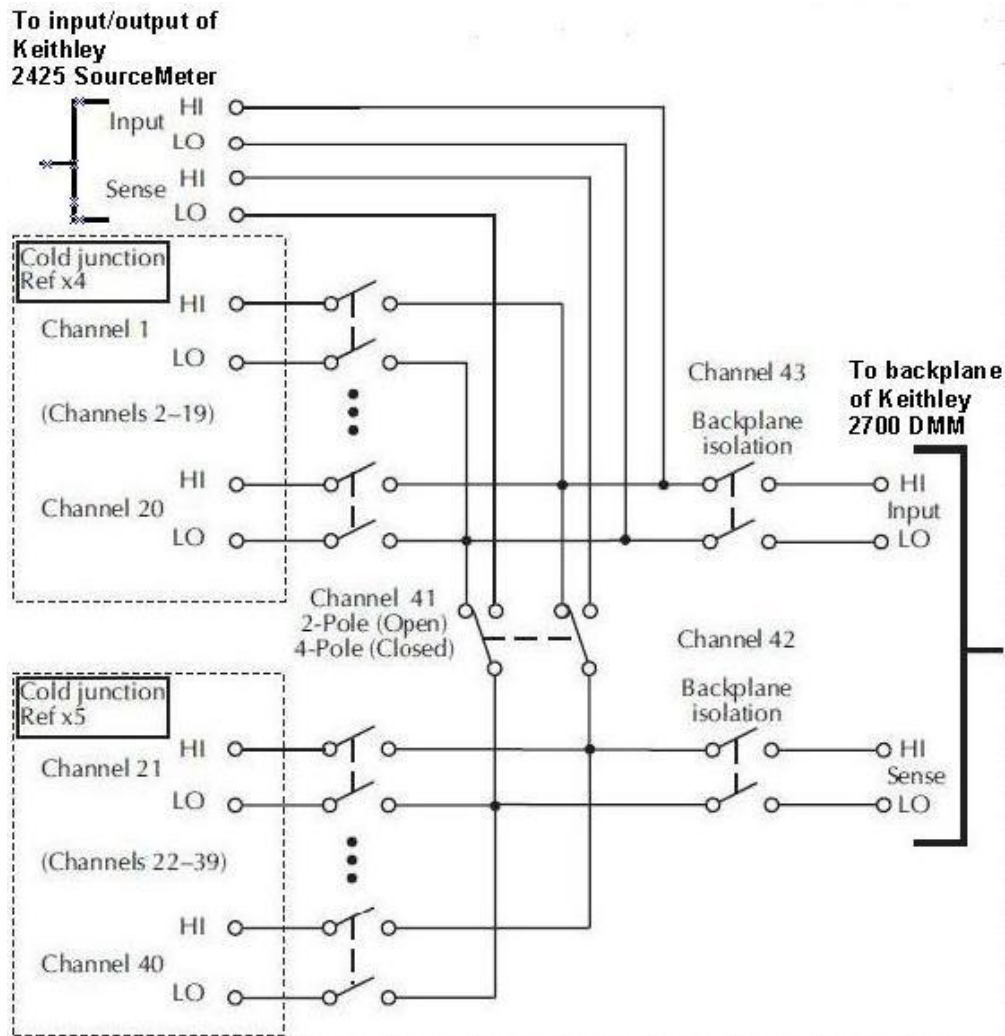


Figure 3.5: Simplified schematic of Keithley 7708 multiplexer.

Channel-41 (2-wire/4-wire configuration), Channel-42 (sense isolation from backplane) and Channel-43 (input isolation from backplane) are normally automatically configured by the Keithley Model-2700 but they can also be manually configured.

Channel-20 is used to monitor the ambient temperature around the T-Sunalyzer by measuring the terminal voltages of the K-type thermocouple. The Keithley Model-7708 includes built-in cold junction compensation (CJC) sensors which can automatically linearize thermocouples, allowing direct connection of thermocouples for temperature measurements. Thermocouples measure the electrical potential at the junction of two different metals, which depends on the temperature. CJC are necessary to compensate for the potential due the junction between each end of the thermocouple and the connector or terminal block of the measuring system [21]. Among the different types of temperature sensors, thermocouples are the most versatile and K-type thermocouples can measure the temperature range of $-200\text{ }^{\circ}\text{C}$ to $1372\text{ }^{\circ}\text{C}$ with $0.001\text{ }^{\circ}\text{C}$ resolution. Their wires can be directly connected to the internal reference junction as shown in Figure 3.6.

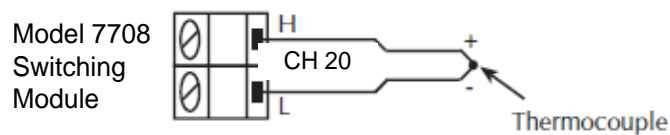


Figure 3.6: Thermocouple connection to internal temperature reference junction.

Channel-19 and Channel-39 are used to check the temperature of the sample (solar cell or module) by using the 4-wire RTD. The 4-wire RTD is the most stable among the temperature sensors. The measurable temperature range of RTD is – 200 °C to 630 °C with 0.01 °C resolution. The connection of RTD to the Model-7708 multiplexer is shown in Figure 3.7.

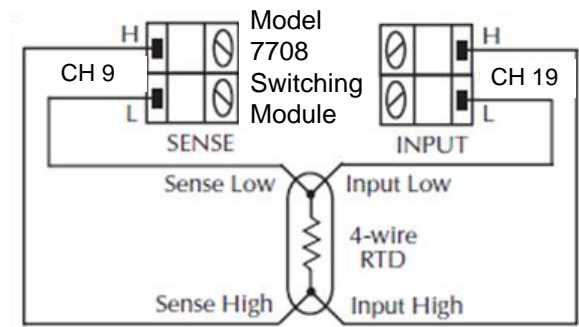


Figure 3.7: 4-wire RTD connection to Keithley Model-7708.

The Keithley Model-7708’s card configuration, performance verification and calibration procedures can be found in the user’s guide [22]. The multiplexing or switching channels are rated as 300 Volt DC and 1 A switched and it is important not to exceed 300 Volt DC between INPUT High and Low terminals of plug-in module or between any adjacent channels.

3.1.2.2 Keithley Model-2700 Digital Multimeter

The Keithley Model-2700 DMM is used to select the channel to be measured by the SourceMeter and is also used to monitor the ambient temperature of T-Sunalyzer and the temperature of the sample. It offers a low-cost alternative to separate DMM and multiplexer or switching system, data loggers and plug-in card data acquisition equipment. The connection of the sample to the DMM with one of the 4-pole switches of the multiplexer is shown in Figure 3.8. For 4-wire measurement, channels 1 to 20 of Model-7708 multiplexer are paired to the channels 21 through 40 and thus channel 16 is also closed when channel 6 is closed.

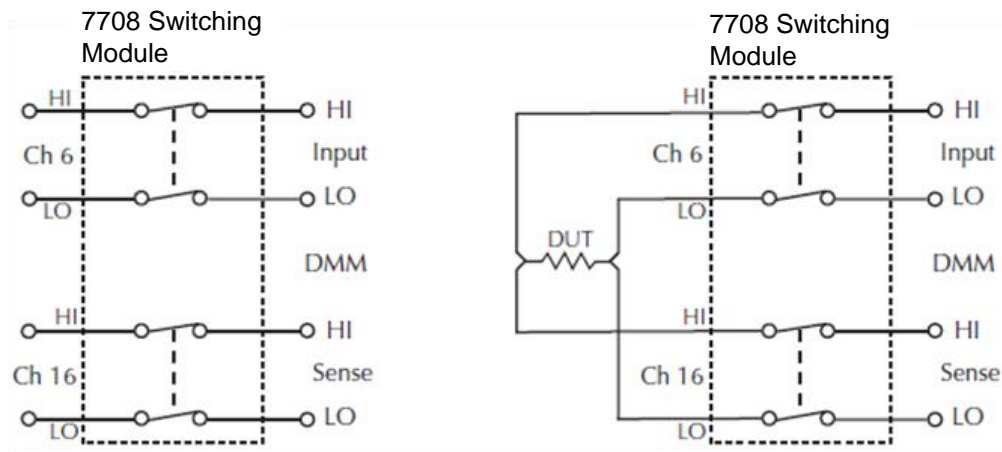


Figure 3.8: Connection to DMM with 4-wire measurement function.

The range of Model-2700 DMM measurement capabilities are DC voltage measurements from 0.1 μV to 1000 V, DC current measurements from 10 nA to 3 A and temperature measurements from -200 $^{\circ}\text{C}$ to 1820 $^{\circ}\text{C}$ respectively. For thermocouples, the temperature measurement range depends on which type of thermocouple is being used. Thermocouples that are supported include types J, K,

N, T, E, R, S, and B [23]. In the *K*-type thermocouple circuit of T-Sunalyzer, the reference junction or the cold junction of Model-7708 is kept at a stable known temperature. The Model-2700 DMM calculates the actual reading at the thermocouple by factoring in the reference temperature. The resistance of the RTD changes with a change in temperature. The most accurate measurement of the low resistance of RTD is achieved by taking a 4-wire resistance measurement with DMM to monitor the temperature of the sample.

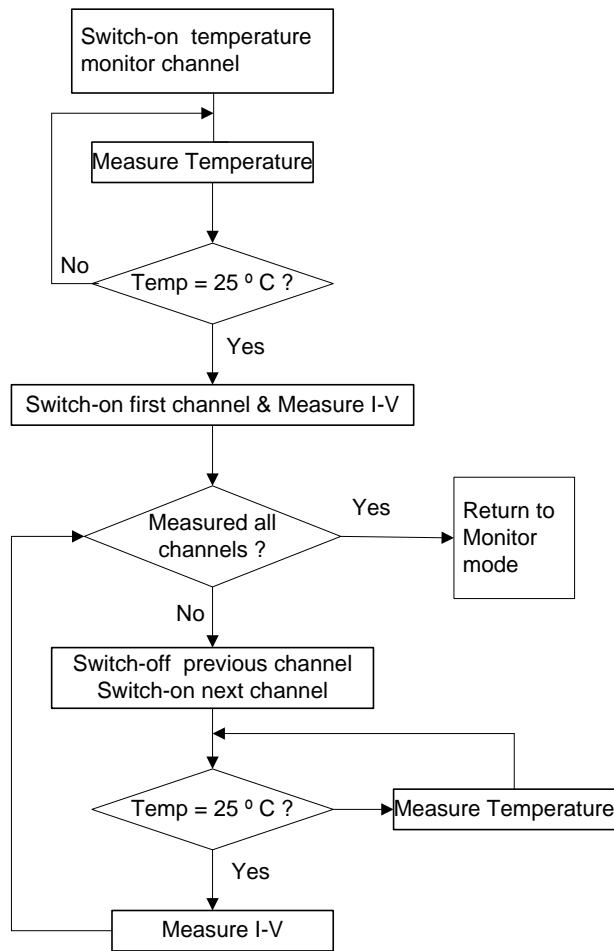


Figure 3.9: Algorithm used in temperature-monitored scanning of DMM.

In the scan mode of Model-2700, a channel can be assigned as a monitor channel. It can be programmed to start scanning each of the enabled channels only when the monitor channel detects that a reading limit has been reached. The channels are scanned from the lowest to highest numbered channel and the disabled channels are not scanned. The temperature monitored by 4-wire RTD is used to trigger the *I-V* measurement. It will start scanning each of the enabled channels for *I-V* measurements only when the temperature reading reaches 25 °C. The algorithm used for this feature is shown in Figure 3.9.

3.1.2.3 Keithley Model-2425 Source Meter

As discussed in Section 2.4.1, using a SourceMeter is the simplest way to characterize the *I-V* curve under illuminated conditions and to capture the reverse bias characteristics of the cell under dark conditions with one single instrument. Moreover, a SourceMeter also eliminates complex synchronization and connection problems that surface from using separate sourcing and measuring instruments. The Keithley Model-2425 SourceMeter is selected for T-Sunalyzer because it provides precision voltage and current sourcing as well as accurate measurement capabilities. The highly stable DC power source characteristics include low noise, high precision and read-back, and the multimeter capabilities include high repeatability and low noise.

The Keithley Model-2425 has 100 W capability in the 1 A range and also offers a 3 A range with 60 W power capability. The source and measurement ranges are shown in Table 3.1. The maximum DC source power is 110 W and the general operating boundaries for the Model-2425 SourceMeter are shown in Figure 3.10.

Table 3.1: Source and measurement ranges of Keithley Model-2425 SourceMeter

| | |
|----------------------------------|-----------------------------------|
| Source DC or pulse voltage range | 5 μ V to 105 V |
| Measurement DC voltage range | 1 μ V to 105.5 V |
| Source DC current range | 500 pA to 3.15 A |
| Measurement DC current range | 100 pA to 3.16 5A. |
| Measurement resistance range | 10 $\mu\Omega$ to 21.1 M Ω |

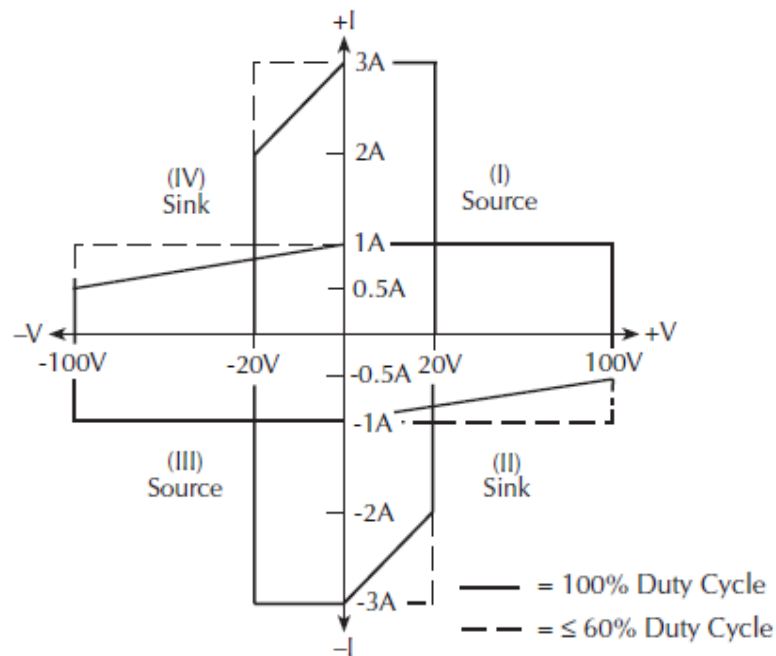


Figure 3.10: Operating boundaries of Model-2425 SourceMeter [25].

The Model-2425 is capable of protecting the sample from damaging by accidental overloads and thermal runaway, etc. The current and voltage sources are designed with programmable and read-back capabilities in order to maximize the device measurement integrity. The source will be clamped at the limit to provide fault protection when the read-back value reaches a pre-programmed compliance limit. The SourceMeter has an over-temperature protection circuit that will turn the output off in the event that the SourceMeter overheats. This condition is indicated by a message and output of SourceMeter cannot be turned on until the SourceMeter cools down.

In the T-Sunalyzer, the I - V characterization of solar cells or modules is accomplished by sweeping the output voltage of Model-2435 SourceMeter from a value which gives I_{sc} to V_{oc} . The Model-2425 can source a voltage or current while making measurements without needing to change connections and it also offers many built-in features that allow it to run complex test sequences with minimum computer control. The solar cells are connected to the Model-2423 SourceMeter through the Model-7708 Multiplexer while each channel to be measured is selected by Model-2700 DMM.

When configured to source voltage as shown in Figure 3.11, the SourceMeter functions as a low-impedance voltage source with current limit capability and can measure current or voltage [25].

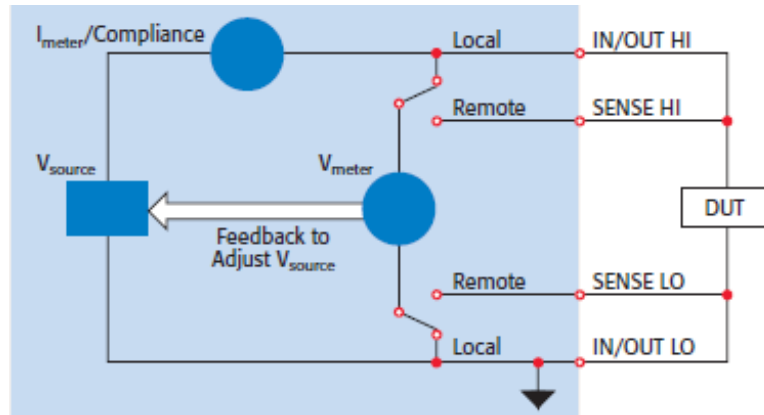


Figure 3.11: 4-wire connection of the sample to SourceMeter.

The sense circuitry is used to continuously monitor the output voltage and make adjustments to the V-Source as needed. The V-Meter senses the voltage at the input/output terminals (2-wire local sense) or at the sample (4-wire remote sense using the sense terminals) and compares it to the programmed voltage level. If the sensed level and the programmed value are not the same, the V-Source is adjusted accordingly. The remote sense eliminates the effect of voltage drops in the test leads ensuring that the exact programmed voltage appears at the sample.

To characterize the I - V curve under illuminated conditions and dark I - V curves at the forward bias region, T-Sunalyzer sources the voltage-steps exponentially from 0 V (I_{sc}) to V_{oc} whereas it sources negative voltage-steps linearly from 0 V to the device breakdown voltage to capture the reverse bias characteristics of the cell under dark conditions. The I - V measurements are taken at each voltage step. The voltage steps are programmed to follow an exponential curve and are also customized to take more measurement points near the maximum power point. The

sourcing and measurement sequence at each step of voltage level is shown in Figure 3.12. The SourceMeter measurement speed itself is optimized for the measurement accuracy and the total time taken depends on the number of measurement points specified by the user for each I - V curve.

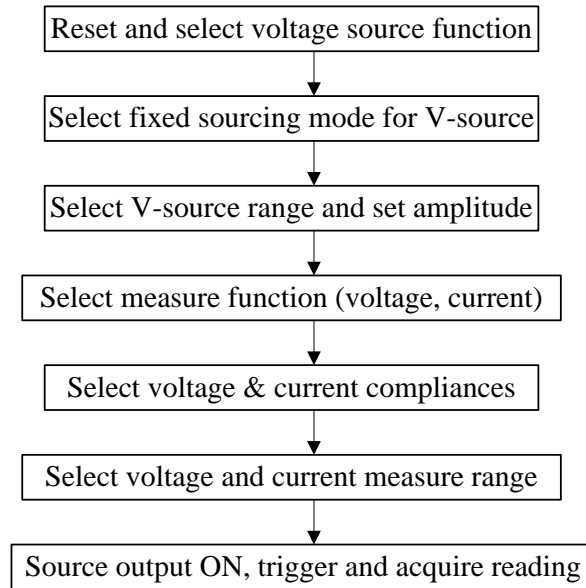


Figure 3.12: Source and measure sequence of SourceMeter.

3.1.3 Xenon light source system

The T-S analyzer uses a continuous illumination with an adjustable light intensity. The illumination is designed in the bottom-up configuration so that the solar cells can be contacted via the upward-facing rear surface and it is easier for the users to align the probes to the contacts. The light source system consists of a single 3 kW xenon lamp, the lamp's holder with the location X-Y-Z adjuster, an ellipse collection mirror or reflector, an integrator lens, plane reflective mirrors and a stable constant current supply for xenon lamp. It is designed to achieve light intensities of 0.001 to

1.2 suns for the sample size of 30 cm x 40 cm by using a divergent beam, light intensity filters and motorized height adjuster for the sample holder.

A shutter is also included to block the light source to the measurement chamber when the T-Sunalyzer is in idle state. The shutter is pneumatically controlled by a Festo guided cylinder (Model-DFM-12-200-B-PA-GF) of 12mm piston diameter and 200mm stroke with flexible cushioning rings or pads on sides, proximity sensor and bearing guide [26]. The recirculating ball bearing guide provides smooth running and high speed guidance for the shutter which is a heat-sink attached to the end of the guided cylinder.

The major parts of the xenon light source system of T-Sunalyzer are shown in Figure 3.13. SHIO's UXL series ozone-free xenon short arc lamp is used in T-Sunalyzer. Its spectral distribution is well balanced in the visible spectrum to resemble daylight. The high gas fill pressure provides high luminance and high luminous efficacy [27]. The continuous light of xenon lamp is the closest reproduction of sunlight and the solar related optical technologies such as integration lens and light filters are added in T-Sunalyzer to improve the spectrum, the light distribution uniformity and control of the light intensity.

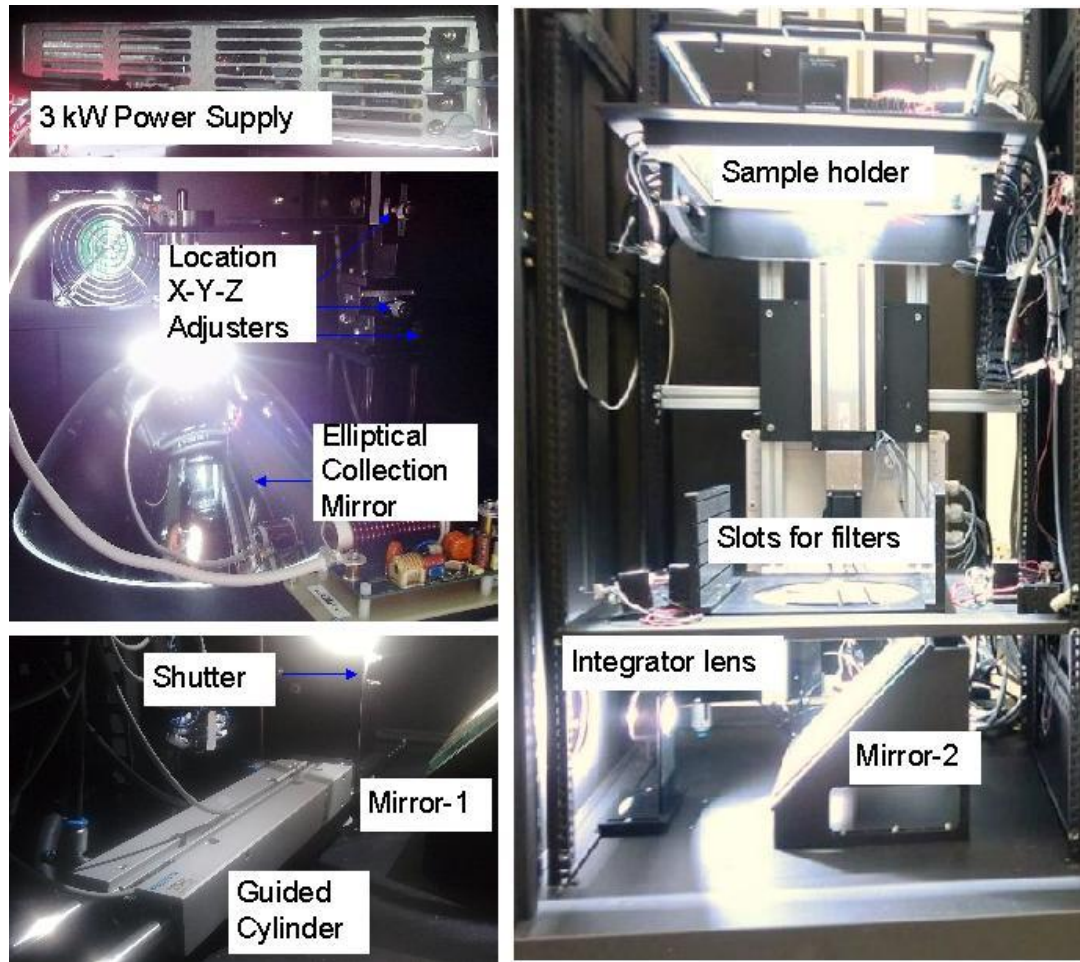


Figure 3.13: Xenon light source and integrator lens in T-Sunalyzer.

Xenon arc lamps have a high internal pressure and can burst during or outside operation potentially causing serious injuries. The user should always wear a protective face mask, leather gloves and protective clothing when handling them and should close the back door of light source system during the measurements. The user must avoid looking directly into the operating lamp as this could cause serious eye injury. T-Sunalyzer keeps track of the total usage of the xenon arc lamp and gives a warning when the rated service life has been reached. When disposing of the lamp,

the used lamp must be placed in its original protective case and original cardboard packaging and cardboard box must be sealed securely with tape before dropping it onto a hard floor from about 3 feet height to break it.

The casing of T-Sunalyzer system is designed to be a light proof enclosure for dark I-V measurements. The Si monitoring cell is used to monitor the light intensity and stability by measuring its output current with the SourceMeter.

3.1.4 Thermally controlled sample holder

The sample holder of T-Sunalyzer is basically 40 cm x 30 cm x 0.5 cm size transparent glass tank with water capacity of 600 ml. The temperature of the sample holder is controlled by recirculating cooling water from a chiller or cooler. The user can set the required water temperature by using the front panel keypad. The cooling water is supplied to the sample holder and is circulated back to the chiller through its outlet and inlet. The tap to control the water flow to the inlets of the sample holder and the tap to control the water flow from the outlets of the sample holder are shown in Figure 3.14.

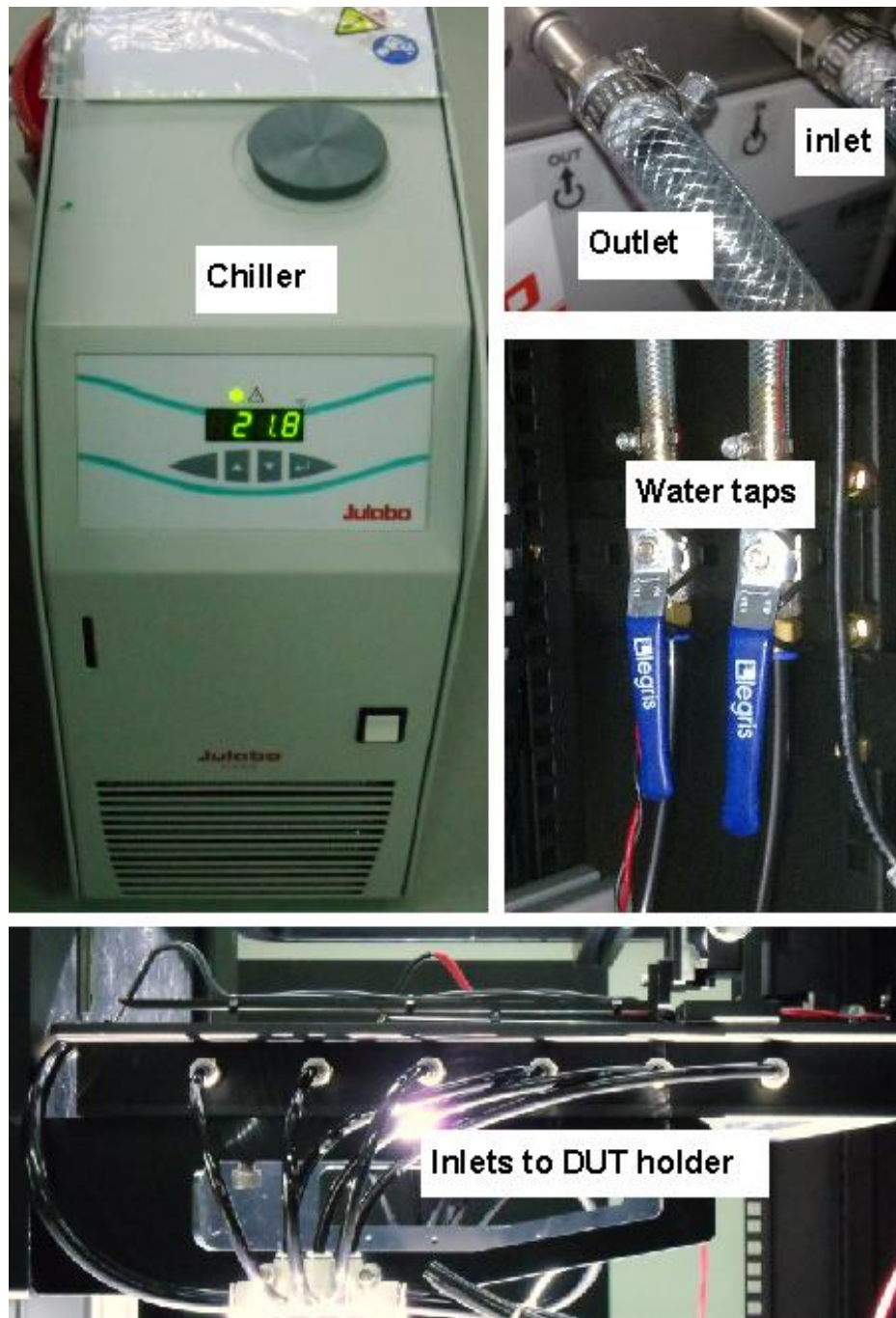


Figure 3.14: Water-cooling temperature control system of the sample holder in the T-Sunalyzer.

The compact recirculating cooler Model-F250 from Julabo is selected for the sample holder for its environmentally friendly operation with low energy consumption. The working temperatures are from 5 °C to 40 °C and it uses PID control to get temperature stability of ± 0.5 °C. It also has excess temperature protection and low water level protection features. A complete shutdown of the compressor and circulating pump occurs when the water temperature has reached the safety temperature of 85 °C or the low water level protection device is triggered and the user will be alarmed. The safety notes and installations, operating procedures, troubleshooting guide, clean or repairing and draining of the recirculating cooler can be referred in the operating manual [28]. The height of the sample holder can be changed by a motorized height adjuster so that *I-V* measurements at different light intensities or variable illumination measurement (VIM) tests can be done with the divergent light beam.

3.1.5 Motorized height adjuster for the sample holder

A motorized height adjuster is used to locate the sample holder at different positions for VIM tests. The compact linear motion system, Model-CKK-15-110, from Bosch-Rexroth and FALDIC-ALPHA5 servo system from Fuji Electronics are integrated together to implement the height adjuster as shown in Figure 3.15.

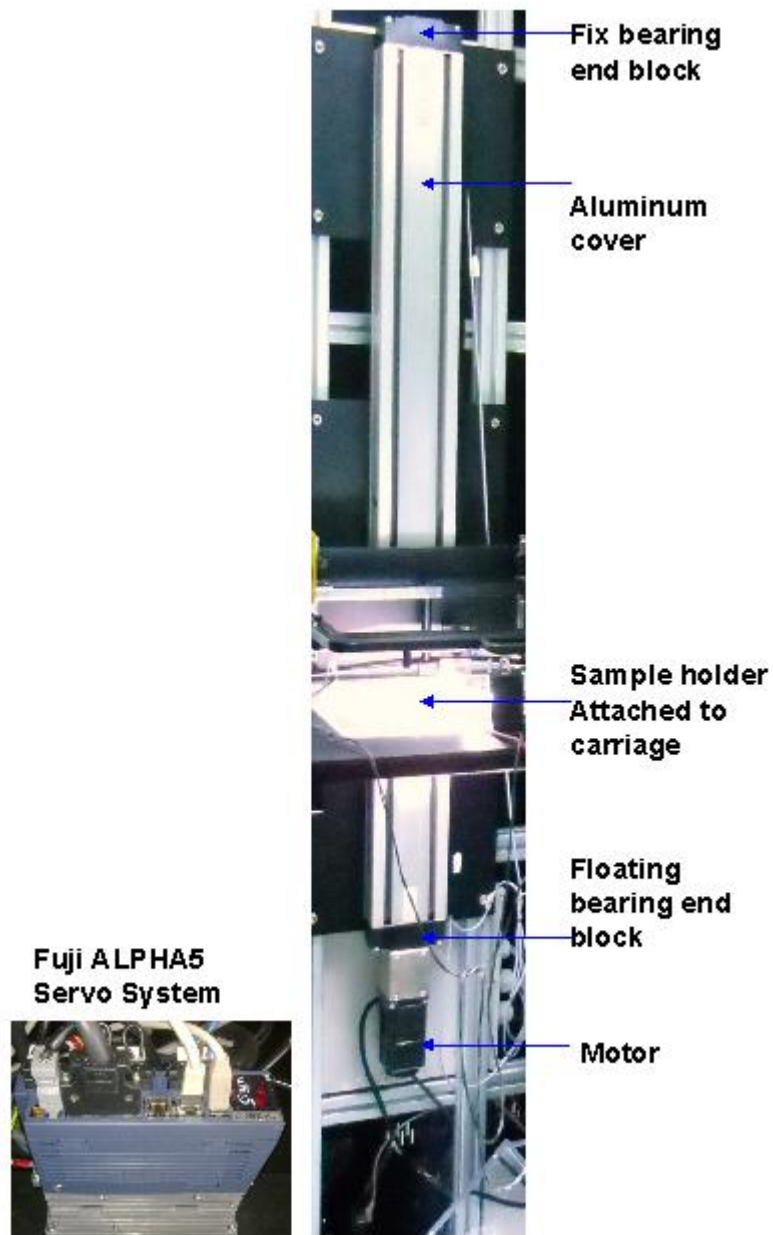


Figure 3.15: Servo system and motorized linear motion system.

Model-CKK-15-110 is a precision readymade linear motion system with ball rail drive [29]. The compact linear motion system includes AC servo drives with integrated brake and attached feedback, motor mount which fastens the motor to the

compact module and also serves as a closed housing for the coupling, mounting duct made of profiled aluminum and integrated zero-clearance ball rail system. The detailed information of mounting the sample holder, installing the drive, maintenance and replacements of assemblies can be found in the manual of CKK compact module [30]. ALPHA5 series is a fast and high accuracy servo system with a short adjustment time during system startup, vibration suppression control and easier maintenance. The specifications of servo amplifier and connections diagram for ALPHA5 can be referred in its application notes [31] and product catalog [32].

3.2 Software

The software of T-Sunalyzer has the ability to directly control the individual building blocks of the system via LAN, USB and RS232 ports of the computer which is integrated with all the necessary I/O cards, operating system and monitor. The measured current and voltage data are analyzed by the T-Sunalyzer software in order to derive the important device parameters such as PV efficiency, open-circuit voltage (V_{oc}), short-circuit current (I_{sc}), short-circuit current density (J_{sc}), maximum power output (P_{max}), voltage at maximum power out (V_{mp}), current at maximum power (I_{mp}), current density at maximum power (J_{mp}), fill factor, 1-Sun series resistance $R_{s.light}$ and $R_{s.dark}$ as a function of current density, shunt resistance and 1-Sun ideality factors as a function of voltage. The software is also able to automatically test and analyze multiple cells in a module according to a required sequence. The cell and ambient

temperatures are monitored to take measurements only at a specified standard temperature.

The integrated calibration feature supports T-Sunalyzer to measure I-V behavior of solar cells and modules under an illumination as close as possible to STC. It ensures that the system is operating at a well-defined light intensity, illumination uniformity and spectral balance. The test conditions can be set as dark, constant illumination, different intensity of illuminations or different temperatures. The measurements are classified into five groups according to the different test conditions: light test, dark test, resistance test, temperature coefficient test and variable illumination measurement test.

3.2.1 Illumination test

The illumination or light test of T-Sunalyzer under standard conditions enables the measurement of the solar cell efficiency. This is the most fundamental characterization parameter used to compare the solar cells and modules from different manufacturing companies and different research technologies in research institutions. The light test of T-Sunalyzer generates $J-V$ and $I-V$ curves and determines the important electrical parameters such as V_{oc} , I_{sc} , J_{sc} , P_{max} , V_{mp} , I_{mp} , J_{mp} , efficiency, fill factor, cell temperature, ambient temperature, light intensity, series and shunt resistances.

3.2.2 Dark test

The current and voltage measurement of solar cells in the dark give valuable information about the diode properties of the device. The minor fluctuations in the light source produce some noise to the measurements and it is difficult to produce the device's diode properties with illumination. In dark I - V measurements, the carriers are injected from a bias voltage compared to photo generated carriers. This gives additional diagnostic information about the device. The dark test of T-Sunalyzer generates J - V curve in both linear and semi-log scales, I - V curve and local ideality factor vs. voltage curve and displays shunt resistance and the area related shunt resistance of the cell.

T-Sunalyzer uses the J - V curve in semi-log scale to derive the ideality factor of the cell at different voltages. In the dark test, the characteristic equation (2.1) can be described by current density

$$J = J_0 \left\{ \exp \left[\frac{qV}{nkT} \right] - 1 \right\}.$$

For the voltages greater than 50 to 100 mV, it can be reduced to

$$J = J_0 \exp \left[\frac{qV}{nkT} \right].$$

By taking log of both sides of the above equation, it gives

$$\text{Log} (J) = \text{Log} (J_0) + \left[\frac{qV}{nkT} \right],$$

so $\left[\frac{q}{nkT} \right]$ is the slope and $\text{Log} (J_0)$ is the interception of the J - V curve in semi-log scale under dark condition.

3.2.3 Resistance test

In the resistance test, T-Sunalyzer generates a J_{sc} - V_{oc} curve and uses it as an R_s -corrected I - V curve in order to determine the dark and illuminated lumped series resistance. $R_{s.light}$ is derived from the shift in voltage between the J_{sc} - V_{oc} curve and illuminated I - V curve in semi-log scale where as $R_{s.dark}$ is determined from voltage shift between the J_{sc} - V_{oc} curve and dark I - V curve in semi-log scale after Aberle *et al.* [33]. The resistance test of T-Sunalyzer generates $R_{s.light}$ and $R_{s.dark}$ curves as the functions of J_{sc} . The local ideality factor curve as a function of voltage is also determined.

3.2.4 Temperature coefficient test

The band gap of a semiconductor is increased or reduced by a decrease or increase in temperature respectively. The main parameter affected by the change in temperature is the V_{oc} of the cell as discussed in Section 2.1.3.8. In the temperature coefficient test of T-Sunalyzer, the user can control the cell temperature and generate I - V curves at different temperatures to analyze the effect of the temperature on the cell. The T-Sunalyzer analyzes how I_{sc} , V_{oc} and P_{max} change with temperature for different irradiance levels and derive temperature coefficients α , β and γ which are the slopes of $\left(\frac{\Delta I_{sc}}{\Delta T}\right)$, $\left(\frac{\Delta V_{oc}}{\Delta T}\right)$ and $\left(\frac{\Delta P_{max}}{\Delta T}\right)$ at STC conditions.

3.2.5 Variable illumination measurement (VIM) test

T-Sunalyzer has a specific evaluation method for thin-film cells based on the variable illumination measurement (VIM). The software of the T-Sunalyzer allows the measurement of the same solar cell at various light intensities by controlling the height of the sample holder. The light intensity can be varied in the range of 1.2 suns down to 0.001 suns by adjusting the distance of the solar cell from the source light and using the optional neutral density filters. The VIM test of T-Sunalyzer allows a quick evaluation of the results by generating V_{oc} , FF , R_s and R_{sh} curves as a function of the current density J_{sc} .

CHAPTER 4: EXPERIMENTAL SETUP AND MEASURED RESULTS

In this chapter, experimental measurements will be presented and discussed to evaluate the performance of T-Sunalyzer for the illumination, dark, resistance, temperature coefficient and variable illumination measurement test. T-Sunalyzer is set up in the PV Characterization lab of SERIS with required facilities such as high current AC power supply and compressed dry air (CDA) supply as shown in Figure 4.1. The xenon light source system is installed in the left most rack in the figure. The power consumed by the solar simulator is shown in kW on the front panel display and the user can adjust it up to 3 kW to generate the required light intensity. The middle tall rack accommodates the integrator lens of solar simulator, the thermally controlled sample holder and its motorized height adjuster. The electronic measuring instruments and the computer with T-Sunalyzer software are installed in the right rack.

The T-Sunalyzer is designed to characterize samples of up to 30 cm x 40 cm in size. Assuming an energy conversion efficiency of 10% this results in 12 W power under STC. It is also customized to measure an array of multiple individual small cells, typically 15 cells with 1 cm² area each. For the purpose of analyzing the functionality and performance of the T-Sunalyzer, the current and voltage measurements presented here are taken with 1 cm² $\mu\text{c-Si:H}$ thin film solar cells with the standard layout used at SERIS. For details on this type of solar cell, the interested reader is referred to the literature [ref].



Figure 4.1: T-Sunalyzer in SERIS's characterization lab.

4. 1 Illumination test

The illumination test is carried out with an irradiance level of 1000 W/m^2 . The integrator lens ensures that the spatial uniformity over the illumination area is better than 5 %. The cell temperature is maintained at $25 \text{ }^\circ\text{C}$ before the start of the measurements. The solar simulator of T-Sunalyzer generates a light spectrum similar to AM1.5 spectrum and thus the measurements are taken approximately under STC. Issues regarding the contact resistance between the probes and solar cell are minimized by using four-wire sensing method.

During the illumination test, the T-Sunalyzer outputs and scans voltages from the user-defined start voltage to the end voltage and also samples the currents at each user-specified voltage point. The measurement results are displayed as J - V , I - V and P - V curves in the graphical user interface of the T-Sunalyzer software and all the related electrical characterization parameters are shown in a table beside the graphs. The measurements raw data are also logged in .csv files and the users can choose data analysis and graphing software such as Microcal Origin to display them in the graphical format of their choice.

The illuminated J - V curve with V_{oc} of 0.411 V and J_{sc} of 10.09 mA was measured by the T-Sunalyzer and is shown in Figure 4.2. The curve shows some unexpected fluctuations due to instability in the light source. The J - V curve follows the shape of a

J - V curve for a diode but shifted by J_{sc} due to the illumination. The current axis is inverted as a convention to show that the solar cell is generating the power. The scanning of voltage steps is programmed to follow an exponential curve to ensure that more measurement points are taken near the maximum power point.

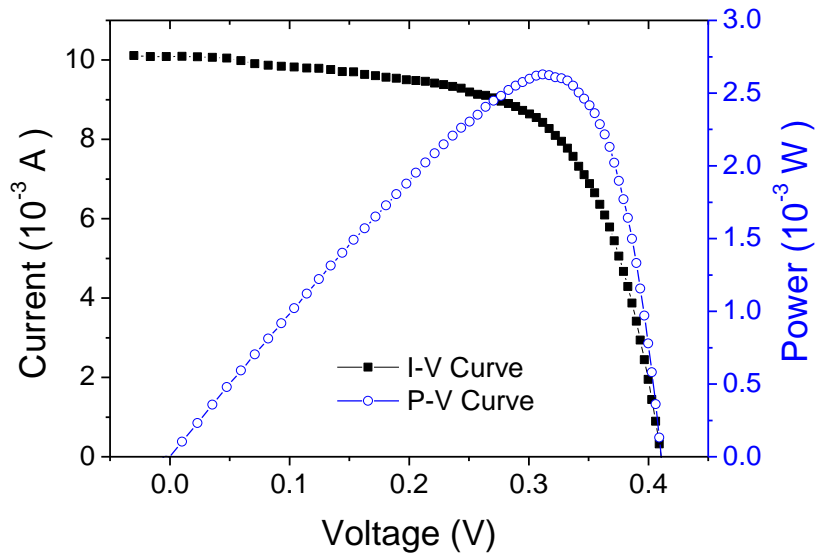


Figure 4.2: Measured illuminated I-V and P-V curves.

T-Sunalyzer also displays the graph of power generated from the solar cell as a function of voltage as shown in Figure 4.2. The illuminated curves allow T-Sunalyzer to determine other electrical characterization parameters such as the efficiency and fill factor of the solar cell by using standard formulae.

4. 2 Dark test

In the dark test, the T-Sunalyzer takes measurements of the cell in an enclosed chamber without illumination. Similar to the illumination test, it steps the voltage steps and samples voltage and current values at each user-defined voltage values. The direction of current flow in the dark test is opposite to that in illumination test and it flows into the solar cell. Negative current values are measured in this case. The dark J - V curve in Figure 4.3 measured by T-Sunalyzer shows the exponential characteristic of the diode as discussed in Section 3.2.2.

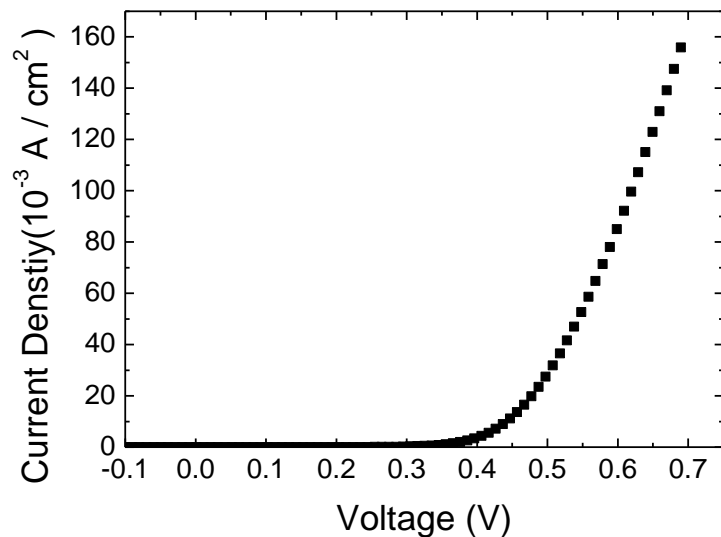


Figure 4.3: Measured dark J - V curve.

The measurements in the dark are not affected by the fluctuations of the light source and the resulting smooth curves show that the customized 4-wire probes and the instruments in electronic measuring module of T-Sunalyzer are functioning adequately.

The linear J - V curve in the dark test is not very useful to analyze the different loss mechanisms of solar cells in the different region of the graphs. The dark J - V curve in a semi-log scale is generated by the T-Sunalyzer as shown in Figure 4.4 to derive the ideality factor of the solar cell from its slope.

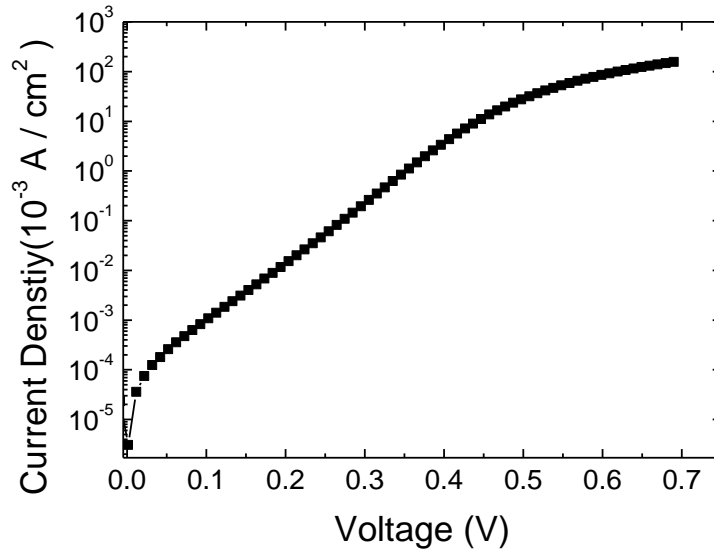


Figure 4.4: Measured dark J - V curve in semi-log scale.

The local ideality factor (n) vs. voltage (V) curve is shown in Figure 4.5. At low and intermediate operating voltages, the ideality factor is constant, as expected for silicon thin-film diodes. The large values of ideality factor at high operating voltages are due to the series resistance (R_s).

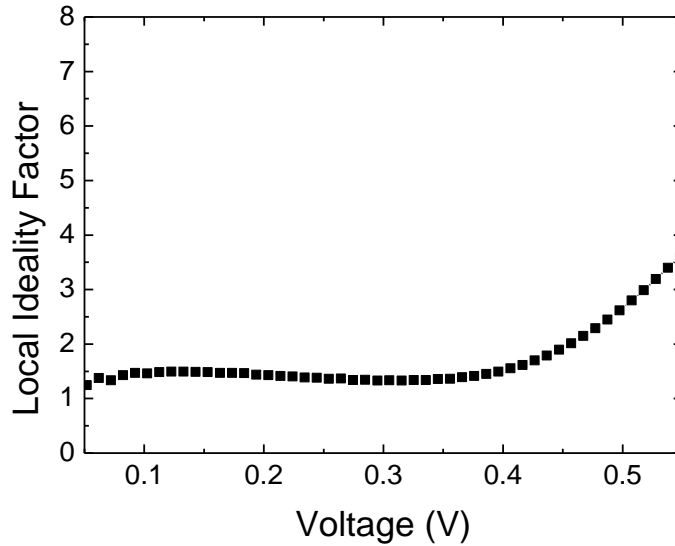


Figure 4.5: Measured dark n - V curve.

4. 3 Resistance test

In the resistance test, T-Sunalyzer generates $R_{s.light}$ and $R_{s.dark}$ curves as a function of the J_{sc} as shown in Figure 4.6. This is also a variable illumination measurement test at different light intensities. It shows that $R_{s.light}$ and $R_{s.dark}$ of this solar cell are dependent on current density flowing in the cell. $R_{s.light}$ decreases with increasing short circuit current density whereas $R_{s.dark}$ increases with increasing short circuit current. The high R_s value contributes to the relatively low 1-sun fill factor of about 63% for the sample under test. A general assessment of the accuracy of using the method discussed in Section 3.2.3 is impossible because it depends on the specific type of PV device under test [33]. The uncertainties of the measurements are minimized by maintaining the sample under STC as close as possible and using the 4-wire measurement method with a high-resolution SourceMeter.

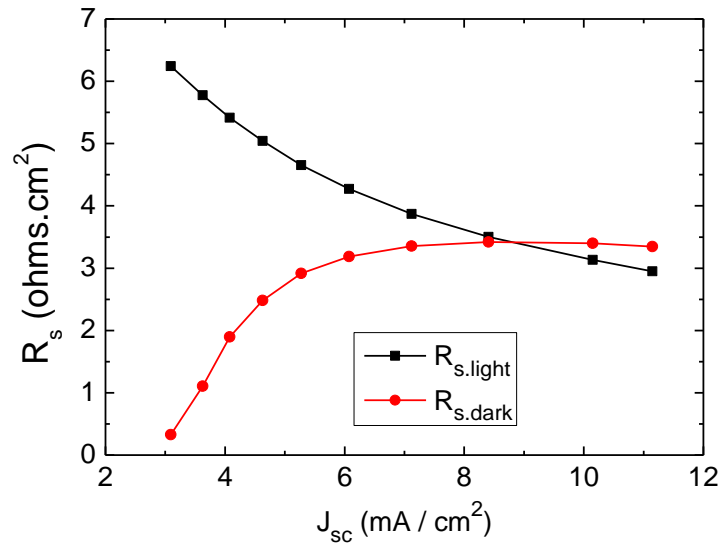


Figure 4.6: Measured $R_{s.light}$ and $R_{s.dark}$ vs. J_{sc} .

4. 4 Temperature coefficient test

The J-V curves measured by T-Sunalyzer at different temperatures are shown in Figure 4.7. The V_{oc} of solar cell decreases whereas the I_{sc} slightly increases with increasing temperature as discussed in Section 2.1.3.7. The output voltage of crystalline Si solar cells reduces by 1.6 mV/K and V_{oc} of the measured solar cell reduced about 3 mV/K with increasing temperature.

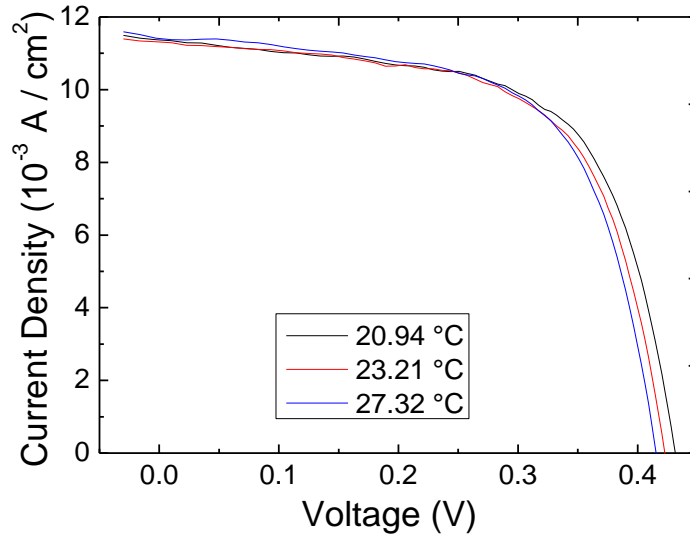


Figure 4.7: Measured J-V curves at different temperatures.

4.5 Variable Illumination Measurement (VIM) Test

In the VIM test, T-Sunalyzer adjusts the height of the sample holder and takes the measurements at 11 different positions. The neutral density filters are not ready to test by the time the VIM measurements are taken for the thesis. The light intensity is about 1.4 suns at the lowest position and about 0.2 sun at the highest position. Since the output power of power supply to the xenon lamp is kept at the same value, the spectrum of the light source is relatively constant during each set of VIM tests. The V_{oc} and fill factor curves as functions of the current density J_{sc} for different light intensities are shown in Figure 4.8 and Figure 4.9 respectively. From these curves, the developer of solar cells gains useful information on the properties of the p-i-n junction and the metallization.

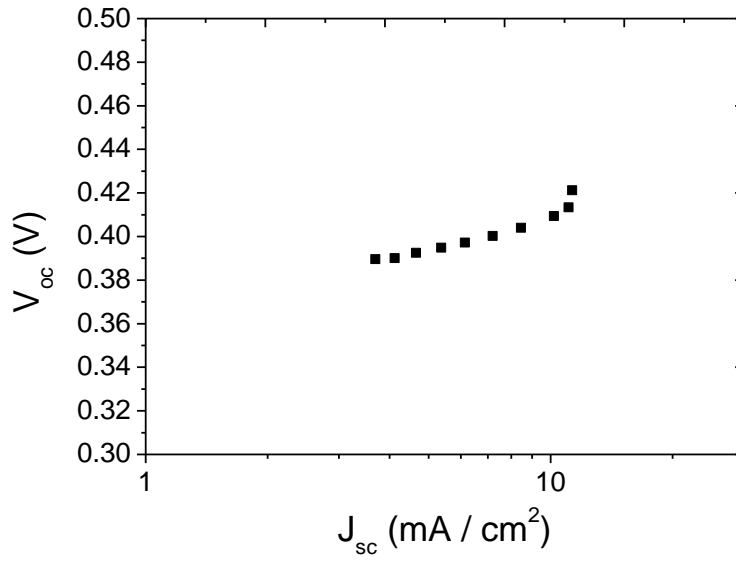


Figure 4.8: Measured V_{oc} - J_{sc} curves at different light intensities in semi-log scale.

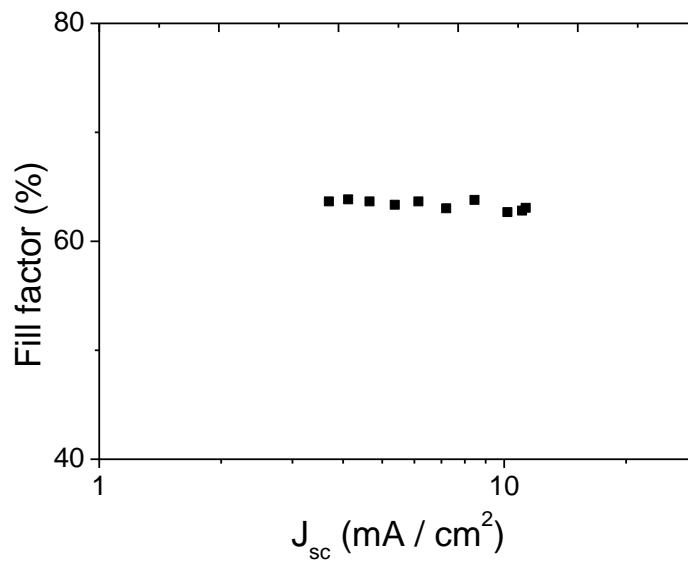


Figure 4.9: Measured FF- J_{sc} curves at different light intensities in semi-log scale.

CHAPTER 5: CONCLUSION AND RECOMMENDTION

In this final chapter, the results obtained from the T-Sunalyzer project are summarized with specific reference to the aims of the project described in the introductory chapter.

5. 1 Summary and implications of measured results

A cost-effective yet highly versatile and powerful *I-V* tester for thin-film solar cells and modules was successfully designed, constructed, and thoroughly tested in this project. The 3 kW xenon light source with a divergent beam gives continuous illumination in the bottom-up direction and is able to achieve light intensity of about 1.1 suns for sample size of 30 cm x 40 cm. With the customized integrator lens, it is able to control the light uniformity within + /- 3 to 4 % for an illuminated area of 30 cm x 30 cm and about +/-7 to 8% for 30 cm x 40 cm area. The light intensity can be adjusted to as low as 0.001 suns by using suitable neutral density filters. The system is also designed with the light proof enclosure for dark *I-V* measurements. T-Sunalyzer is equipped with a lamp which can give a very close reproduction of sunlight. The cost for this in-house design solar simulator is very low compared to other simulators of similar performance available in the market.

The wide range of available light intensities allows T-Sunalyzer to take J_{sc} - V_{oc} curves of the sample and thus is able to determine accurate measurements of $R_{s.light}$ and $R_{s.dark}$ at different external current densities. The VIM test feature is another advantage of T-

Sunalyzer that gives a better insight into solar cells by generating V_{oc} , FF , R_s and R_{sh} curves as functions of the current density J_{sc} . T-Sunalyzer is able to measure in the -100 V to 100 V and -3 A to 3 A range. It has 100 W and 60 W measurement capabilities in the 1 A and 3 A ranges respectively.

The solar cell or modules can be placed up-side down onto a transparent sample holder with an illuminated area of 30 cm x 40 cm and the front glass of the samples is facing downwards. In this way it is more convenient for the user to align the 4-wire probes to the back contacts of the thin-film solar cells or modules. The circulating cooling water through the transparent sample holder allows T-Sunalyzer to keep the sample temperature at a user-defined value in the range of 5-40 °C. The sample temperature is monitored to take measurements only at the desired temperature. The Si monitoring cell is also kept at the same temperature as the sample. The position of the sample holder is adjustable with motorized and programmable height adjuster with position accuracy of 1 mm and load capacity of more than 100 kg. The movement of the sample holder is very smooth without vibrations and can be controlled and programmable to the required height in order to use a suitable light intensity for tests.

The probing mechanism of T-Sunalyzer allows characterizing thin-film modules with a size of 5 cm x 5 cm to 30 cm x 40 cm. The customized probe bars based on SERIS' cell layout and the single-axis adjustable micro-probes enable T-Sunalyzer characterizing multiple cells at the same time.

The control, data acquisition and data analysis software of T-Sunalyzer can directly control the individual system modules and is able to automatically test and analyze multiple cells in a module according to the required sequence. The light, dark, resistance, temperature coefficient and VIM test are the most versatile features available only in T-Sunalyzer as all-in-one system compared to other simple I - V testers available in the market. The light J - V , I - V and P - V curves, the linear and semi-log J - V curves, I - V and n - V curves in the dark test, $R_{s.light}$ and $R_{s.dark}$ vs. J_{sc} curves in the resistance test, I - V curves at different temperatures in temperature coefficient test, V_{oc} , FF , R_s and R_{sh} vs. J_{sc} curves in VIM test and the characterization of electrical parameters generated by T-Sunalyzer are all specifically designed for productive and efficient research work in optimizing thin-film solar cells as well as for testing them in production lines during the manufacturing process.

The first measurement results from the first prototype showed that T-Sunalyzer has successfully fulfilled the targeted objectives of the project within a reasonable budget. The in-house design not only reduces the overall system cost for SERIS but also gives the flexibility to customize and upgrade system configuration according to the future needs. T-Sunalyzer will hopefully contribute as a very useful and important thin-film I - V tester for the PV community to facilitate the faster growth of the PV industry.

5.2 Recommendations for future work

Though T-Sunalyzer meets all the pre-defined major specifications, some minor issues should be further investigated and improved in the future. According to the solar simulator classification criteria listed in Table (2.1), the performance of the xenon light source system in T-Sunalyzer is between that of class-A and class-B. For a better standard, it can be further optimized. The spectral match can be optimized by adding an AM1.5 filter near the integrator lens.

The spatial uniformity over the illumination area can be improved by redesigning the integrator lens based on experience from the first prototype or the introduction of additional filters after the integration lens. The new design should focus on achieving a more divergent beam which covers a larger measurement area when the sample holder is at its lowest position and the light intensity at its highest position is much lesser comparatively. The light $J-V$ curve is not very smooth due to some noise from fluctuating light which goes to the sample holder without passing through the integrator lens. It is observed that the frame of the integrator lens, shown in Figure 3.13, is too small to block the scattered light. Lower noise data is expected after the size of the frame is improved. The temporal stability or stability over time can be improved by using only the light beam which passes through the integrator lens. With these improvements, the solar simulator of T-Sunalyzer would meet class-A criteria.

Another issue observed is that xenon lamp's power supply is currently automatically shutting down due to the heat up if it is used its near maximum rating of 3 kW. DC fans are used to keep this power supply under suitable temperature. But, the DC fans are not powerful enough and industrial standard AC blowers should be used instead for this purpose. The necessary fixes and improvements for xenon light source system have been discussed and planned with the contractor company.

Although the current recirculating cooler for sample holder is good enough to keep the cell or module temperature at the required STC temperature of 25 °C during the measurements, it takes some time to change the temperature for the measurements during temperature coefficient tests. A more powerful cooler is suggested for more efficient measurements. The sample holder needs to be placed at lowest position before shutting down the T-Sunalyzer in order to prevent air bubbles forming inside it. The air bubbles are still inevitable sometimes when the recirculating cooler is shut down and there is a significant temperature change in the sample holder. Although the bubbles can be taken out before using the T-Sunalyzer again, the current assembly is not that easy to turn the sample holder in vertical position. The mechanism design of sample holder and its frame should be improved so that it can be turned 90° easily in case there is air bubble formed in it due to unforeseen conditions. The dynamics of the probing mechanism and electronic measuring instruments should also be further investigated and improved. It can help to achieve more accurate and reliable current and voltage measurements. By adapting the design for even higher throughput

measurements in the next version of the system, T-Sunalyzer should be able to sell as market product to other thin-film module manufacturers.

REFERENCES

- [1] S. Ladislaw, K. Zyla, J. Pershing, F. Verrastro, J. Goodward, D. Pumphrey, B. Staley, "A Roadmap for a Secure, Low-Carbon Energy Economy", Center for Strategic & International Studies (CSIS), pp. 4-12 (2009), <http://csis.org/publication/roadmap-secure-low-carbon-energy-economy>.
- [2] A. Blakers, P. Devine-Wright, D. L. Gazzoni, A. G. Hestnes (vice Chair), E. Kituyi, J. Kretzschmar, J. Luther (Chair), J. Manwell, H.S. Mukunda, C. Rolz, J. Skea, E. Volkov, W. Zhifeng, M. Yamaguchi, "Research and Development on Renewable Energies – A Global Report on Photovoltaic and Wind Energy", International Science Panel on Renewable Energies (ISPRES), pp. 1-3 (2009), http://www.seris.sg/site/servlet/linkableblob/main/3154/data/ISPRES_report_122009_Lu-data.pdf.
- [3] Aberle, A.G., "Thin-film solar cells", Thin Solid Films, 517 (17), pp. 4706-4710 (2009).
- [4] Green, M.A., "Consolidation of thin-film photovoltaic technology: The coming decade of opportunity", Progress in Photovoltaics: Research and Applications, 14 (5), pp. 383-392 (2006).
- [5] Aberle, A.G.; Lauinger, T.; Bowden, S.; Wegener, S.; Betz, G.; "SUNALYZER-a powerful and cost-effective solar cell I-V tester for the photovoltaic community", Photovoltaic Specialists Conference, 1996., Conference Record of the Twenty-Fifth IEEE, pp. 593 – 596 (1996).
- [6] Granek, F., Zdanowicz, T.; "Advanced system for calibration and characterization of solar cells", Opto-electronics Review 12 (1), pp. 57-67 (2004).
- [7] Mao Meiqin; Su Jianhui; Liuchen Chang; Peng Kai; Zhang Guorong; Ding Ming; "Research and development of fast field tester for characteristics of solar array" Electrical and Computer Engineering, 2009. CCECE '09. Canadian Conference on 3-6 May 2009, pp. 1055 – 1060 (2009).
- [8] Keogh W.M., Blakers A.W., Cuevas A.; "Constant voltage I-V curve flash tester for solar cells", Solar Energy Materials and Solar Cells, 81 (2), pp. 183-196 (2004).
- [9] Keogh, W.; Cuevas, A.; "Simple flashlamp I-V testing of solar cells", Photovoltaic Specialists Conference, 1997., Conference Record of the Twenty-Sixth IEEE, pp. 99 – 202 (1997).
- [10] Keith Reid McIntosh, "Lumps Humps and Bumps: Three Detrimental Effects in the Current-Voltage Curve of Silicon Solar Cells", PhD thesis, University of New South Wales, Australia, pp. 1-24 (2001).

- [11] Eduardo Lorenzo, "*Solar Electricity: Engineering of Photovoltaic Systems*", Progensa, (1994).
- [12] Jenny Nelson, "*The Physics of Solar Cells*", Imperial College Press, (2003).
- [13] PV Education: <http://www.pveducation.org/pvcdrom>
- [14] Fill factor:
<http://www.pveducation.org/pvcdrom/solar-cell-operation/fill-factor>.
- [15] Solar Cell and Module Testing:
<http://cp.literature.agilent.com/litweb/pdf/5990-3262EN.pdf>.
- [16] Characterizing the I-V Curve of Solar Cells and Modules:
<http://cp.literature.agilent.com/litweb/pdf/5990-4050EN.pdf> .
- [17] PV education: <http://www.pveducation.org/pvcdrom> .
- [18] Guidelines for PV Power Measurement in Industry
http://re.jrc.ec.europa.eu/esti/docs_en/EUR-24359-EN.pdf .
- [19] Four-terminal sensing:
http://www.allaboutcircuits.com/vol_1/chpt_8/9.html.
- [20] Probe selection guide: <http://www.qatech.com/tech/catalogs/Selection.pdf>.
- [21] Information on Cold Junction Compensation (CJC) sensors
<http://digital.ni.com/public.nsf/allkb/D2692747F02DDBE786256E8E0024475B>.
- [22] Keithley 7708 40-channel Differential Multiplexer Module
<http://www.keithley.com/products/switch/rfmicrowave/?mn=7708>.
- [23] Model-2700 DMM, Data Acquisition, Data logging System with 2 Slots
<http://www.keithley.com/products/data/datalogger/?mn=2700>.
- [24] Selector Guide for Keithley Digital Multimeters:
<http://www.keithley.com/data?asset=480>.
- [25] Model-2425 100W SourceMeter with measurements up to 100V and 3A
<http://www.keithley.com/products/dcac/currentvoltage/highcurrent/?mn=2425>.
- [26] Festo Guided cylinder DFM
http://www.festo.com/pnf/en-sg_sg/products/catalog?action=partlist&key=570554.
- [27] USHIO Xenon Short Arc lamps
<http://www.ushio.com/products/entertainment/xenonshortarc-uxl.htm>.
- [28] Julabo-F250 Compact Recirculating Cooler/EcoChiller

http://www.julabo.com/us/p_datasheet.asp?Produkt=F250.

- [29] Lear Modules and Cartesian Systems: CKK Ball Screw Driven Compact Modules
http://www.boschrexroth.com/country_units/america/united_states/sub_websites/brus_dcl/Products/Linear_Modules_and_Cartesian_Systems/ckk/index.jsp.
- [30] Linear System Manuals: CKK Compact Modules Manual
http://www.boschrexroth.com/country_units/america/united_states/sub_websites/brus_dcl/a_documentation/lt_manuals/linear_systems/manual_ckk.pdf.
- [31] Fuji Servo System: FALDIC ALPHA5:
http://www.fujielectric.com/fes/products_services/power_drive/sv/download/catalog/MEH555c.pdf.
- [32] High-performance Servo System: ALPHA5 Series
<http://www.fujielectric.com/company/tech/pdf/54-01/FER-54-01-016-2008.pdf>.
- [33] A.G. Aberle and S.R. Wenham and M.A. Green, "*A new Method for Accurate Measurements of the Lumped Series Resistance of Solar Cells*", Proceedings of the 23rd IEEE Photovoltaic Specialists Conference, pp. 113-139 (1993).